Response to Reviewers
August 2019

All reviewer comments appear in *italic text* below, while authors' responses appear in blue text. Line numbers referenced in the authors' responses refer to the revised document.

Response to reviewer 1

Dear Anonymous Reviewer 1,

We appreciate your thoughtful feedback. It helped us to improve the manuscript. Below we comment on your suggestions in detail.

The authors present a statistical analysis of wind power of four wind turbines and wind direction shear, measured using a nearby Lidar. They discriminate between clockwise and counter-clockwise wind direction shear and show a correlation between under performance of the wind turbine and mean directional wind shear. This under performance is primarily visible for lower wind speeds. In general, the paper is very well written. Introduction, choice of data and statistical analysis are clear. The figures are suitable to present the data. My comments are therefore very minor asking for some clarification and some improvements of text and figures. I recommend that the paper is accepted after minor revisions.

General comments

The fact that turbine performance decreases by more than 15% for strong wind shear conditions is very relevant; I can clearly see that. I found the fact that is mostly high veering that is related to a drop in normalized power very interesting. However, I was missing any attempt for a physical explanation on why high veering has such a strong effect whereas high backing does not show the same signal. It seems that you are too defensive here, and a little bit of speculation could be appropriate in the discussion.

Thank you for giving relevancy to our findings. We agree that we did not provide a physical explanation on why high backing does not show a drop in normalized power. To provide a robust and defensible explanation, we would have liked to have a greater number of strong backing cases so that we could develop a rigorous hypothesis. Unfortunately, as we pointed out, an insufficient number of large backing cases occurred so we could not conclusively draw any conclusions regarding its effect on turbine performance. In the updated version of our manuscript, we examine in more detail the effects of small veering and small backing on normalized performance and found similar results for each scenario. We speculate that the variations in available power through the rotor disc and in turbine blades' efficiency are not significant for these subtle wind direction changes (see p. 21, lines 30 – 34; p. 22, lines 1 – 2).

Furthermore, I wonder if the unit deg m^{-1} is indeed the right one in this context. In my opinion, it depicts a certain generality that cannot be drawn from your dataset, given that you looked only at four wind turbines with the same rotor diameter. Given that directional shear is not linear, this may be relevant. Multiplying by 80 and using deg D^{-1} may help to communicate this important limitation.

We carefully considered this thoughtful suggestion, but literature regarding the effects of wind direction shear on turbine performance (e.g. Rareshide et al., 2009; Wagner et al., 2010; Walter et al., 2009) and characterization of the lower boundary layer for wind energy applications (e.g. Bodini et al., 2017)

generally employs this unit. Further, comparisons made with other studies are easier to understand when maintaining the same units. Therefore, we deem appropriate using deg m^{-1} for characterizing shear in wind direction. We also consulted with colleagues using veer in their wind turbine control algorithms, and they specifically requested deg m^{-1}.

Third, I found that the directional wind shear is a function of height was overlooked in the analysis. This fact is clearly stated in the beginning but is ignored later on and only average directional shear is analysed. I wonder especially, what the effect of misalignment (with respect to the ideal 90 degree angle) would be if this misalignment is primarily below or above hub height. Given that wind speed generally increases with height, this seems important. You probably lack data on rotor orientation, but could you expand on this point in the discussion nonetheless? Splitting the analysis to the levels 40-80 and 80-120 may provide some insight.

Thank you for your comment. We considered your suggestion, but as is stated at the beginning of the manuscript, the main objective of this paper was to determine if direction wind shear across the whole rotor layer affects turbine performance to see if this phenomenon might have played an important role in conflicting results regarding the effects of atmospheric stability on turbine operation. If this overall veer did not show interesting results, then breaking it up into 40-80m and 80-120m segments likely would not have done so either. Hopefully our manuscript can motivate more detailed investigations using observations or simulations.

Finally, the rotation direction of the rotor is one asymmetry that may be of relevance given that you found such a distinct difference between veering and backing. Any thoughts?

Thank you for highlighting this as it most certainly plays an important role for large veering and backing scenarios. However, as stated above, we had insufficient large-backing cases to draw conclusions and make a more detailed comparison with turbine performance taking place during large-veering atmospheric conditions. Moreover, we did not expand on this topic as we found small veering and small backing to have similar effects on turbine operation (see p. 17, lines 9 – 18; p. 21, lines 30 – 34; p. 22, lines 1 – 2). The reviewer may be interested to see an investigation of the interactions of veering with wind turbine rotation direction and the effects on turbine wake structure, Englberger et al. (2019), at https://www.wind-energ-sci-discuss.net/wes-2019-45/.

Specific comments

1. Section 2.4: Do you really need a section of its own for two sentences? Furthermore, you mention that you average over 10 minutes in line 16, page 7 as well.

We agree that we did not present information in the best possible way. We have now clarified information in this subsection and expanded it. One of these expansions was to accommodate another reviewer's request for information on time synchronization between turbine and lidar data. Also, we consider it important to explain that lidar data is logged every 2 minutes (2-min averages), and turbine data is logged every 10 minutes (10-min averages) by their data-acquisition systems. Therefore, we match turbine-measured power operation to lidar-measured atmospheric conditions by averaging five 2-min lidar recordings. The text now reads as follows: "Turbine- and lidar-recorded data are averaged over different time intervals by their respective data-acquisition systems (2-min for lidar, and 10-min for turbine). Matching turbine performance with atmospheric conditions was performed by averaging 2-min lidar measurements for the corresponding 10-min turbine power production period. For example, turbine data for July 04, 2013 from 0500 to 0510 LT is matched with the average of five 2-min lidar data measurements corresponding to the same date and time period".

2. Page 15, line 13: Mentioning Turbine A-D comes a little bit out of the blue at this point because this is the very first time the text and the only other reference is Figure 1. You should refer to Figure 1 in this context.

Thank you for pointing this out, we did so in our updated version of our manuscript.

3. Figure 12: I found it confusing that there are four entries in the legend, but only three lines. You write in the text that bins with less than 30 data points are discarded, but I recommend removing the entry for high backing. Furthermore, it is rather strange that the error bars for the low veering case are not bold and black. It is a minor issue, but your readers should not play a guessing game. I have similar issues with Figs. 11 and 13, having four lines, but only 2 legend entries (specifically referring to the median).

Thank you for your comment. We agree that figures should be as clear as possible for the readers. We have included corresponding legends to all our new figures in the updated version of our manuscript.

4. Figure 2: The shading in this plot style leads to three colors in the graph, while there are only two in the legend. It is only a very, very minor remark, but wouldn't a simple line plot do a better job in communicating data availability?

Thank you for this suggestion. We considered a line plot for the updated version of our manuscript but preferred a bar graph. However, we have now separated data availability for turbines and lidar observations to avoid overlapping colors.

Typos

1. *Page 8, Equation 1: Full stop instead of comma after the equation.*

   We appreciate this comment and updated the manuscript accordingly.

2. *Page 15, line 7: 'was on average' instead of 'was in average'*

   We appreciate this comment and updated the manuscript accordingly.

3. *References For Rajewski et. al 2016 and Muñoz-Esparza et.al. 2017, it seems that there are some personal comments that have slipped from the .bib file into the references. The all-caps text is not part of the actual reference.*

   We appreciate this comment and updated the manuscript accordingly.

4. *Figures 11,12,13: You are using "Wind Speed in the x-label here, but "Wind speed everywhere else.*

   Thank you for catching this. We have updated axes labels in every figure and only left the first word of each label with an initial capital letter.

Response to reviewer 2: Rozenn Wagner

Dear Dr. Wagner,

We highly appreciate your feedback. It helped us to improve the manuscript and strengthen our findings. You highlighted some crucial points that were overlooked in our initial manuscript.

General comment

Interesting topic. There is definitely a need for studying and publishing on the effect of veer on wind turbine power performance. However the usual challenge with experimental data is how to identify whether the effect on the performance is due to veer or other wind conditions, especially speed shear which is very much correlated with veer. This is my main criticism to the paper: all the observed performance variations are attributed to the veer effect without considering the speed shear during the measurement campaign. This could totally invalidate the results. A description of the shear during those measurements and an estimate of its expected effect on the turbine performance need to be included in the paper.

Apart from that, the paper is rather well structured. References are made to the relevant existing study on the matter. The analysis and interpretation of the results need to be clarified in several places but this probably only a matter of sharpening the language (see detailed comments).

Thank you for outlining the importance of studying the effect of direction wind shear on turbine performance. We agree that we did not cover the effect of speed shear on turbine operation in the first version, attributing performance variations solely to wind veer. We expanded the Results section to include speed shear characterization (subsection 4.1) following the same methodology as with direction shear. We also included the effects of speed shear on turbine performance (subsection 4.2) by segregating turbine operation according to speed and direction wind shear atmospheric conditions. Later on, in section 5, we further discuss our measurements in contrast to the results and findings of other studies and simulations. We feel these changes have improved the insights available from this dataset.

Detailed comments

P3- l.9: could you clarify this sentence or paragraph? Do you mean in Vanderwende, it was not complex terrain contrary to the two other studies, or it was complex terrain in all of them – then why does complex terrain prevents the occurrence of changing wind direction wind height in the two first cases and not in the other?

Thank you for pointing out we needed to be more specific here – this apparent contradiction is what drove the development of this paper. In Vanderwende and Lundquist, complex terrain was situated nearby but did not channel the flow into the wind turbines. A clarification has been added to the manuscript. The manuscript reads now as follow: “The Wharton and Lundquist (2012a,b) wind turbines, and St. Martin et al. (2016) testing site were surrounded by complex terrain that steered a channeled flow into the turbines and prevented the development of directional wind shear during stable conditions. In contrast, at the Vanderwende and Lundquist (2012) location, complex terrain did not prevent the occurrence of a changing wind direction with height.”

P3-l.22,24 and 25: wrong cross ref: “section 0”

We appreciate this comment and updated the manuscript accordingly.

P4, l3-4 The data have also been used...LES models" – delete this sentence. It is not relevant in the context of this study.

We included this information to give context of the wide variety of studies that stemmed from the CWEX-13 campaign. We decided to keep the reference to this work but moved this sentence further up in the paragraph near references to low-level jet and wake variability studies.

P4- Figure 1: where is this sub-region located in relation to the overall 200 turbines wind farm? Are there any turbine or any obstacles to the south of that region? How far?

Thank you for asking about this issue as any upwind obstacles would have affected turbine inflow conditions. We changed the schematic diagram of the region of interest in the CWEX-13 campaign and in this study to show its location in relation to the overall 200 turbines wind farm and to show topography near turbines (refer to Figure 1 in the updated manuscript). No obstacles are located to the south of the region of interest.

P5, l8: why have you used 2-min averages and not 10 min?

The lidar data was recorded as 2-min averages for other purposes, to aid in meteorological studies of cold front passages and other transient phenomena. For the present work, we simply average 2-min data from the lidar over their respective 10-min turbine operating periods.

P5, fig.2: how were the availability calculated for the lidar and turbine? Availability of 2 min data over one day? At what height for the lidar? For which turbine? Four turbines were mentioned in figure 1? Were the data for wind speed below 2.5m/s also excluded from the lidar data for availability quantification?

We appreciate this comment and the opportunity to clarify the method for calculating data availability, expanding subsection 2.2 and extending Figure 2. Lidar data availability corresponds to lidar-operating time throughout the whole day. It was calculated as availability of 2-min observations of 80-m wind speeds over the whole day (24 hours). Turbine data availability was calculated as availability of power observations for nacelle-measured wind speed above 2.5 m s^{-1}. Turbine data availability showed in Figure 2 corresponds to the mean data availability of the four turbines. Subsection 2.2 has been updated to include this clarification, and data availability in Figure 2 has been divided to show lidar data availability scaled in hours, and turbine data availability in percentage of power measurements recorded for wind speeds above 2.5 m s^{-1}.

P7, fig. 4: those data are from which of the 4 turbines highlighted in Fig 1?

We have added clarification in Figure 4 caption stating that data corresponds to power and blade pitch angle measurements of the four analyzed wind turbines.

P7, section 2.4

1. *This is a bit confusing since it is stated in page 5 that the study was based on 2min averages. Could you please clarify?*

We agree that it seems confusing, so we explained that to determine atmospheric conditions for each 10-min power recordings we averaged the 2-min lidar data over the corresponding power production period and we added a short example. The text now reads as follows: "Turbine- and lidar-recorded data are averaged over different time intervals by their respective data-acquisition systems (2-min for lidar, and 10-min for turbine). Matching turbine performance with atmospheric conditions was performed by averaging 2-min lidar measurements for the corresponding 10-min turbine power production period. For example, turbine data for July 04, 2013 from 0500 to 0510 LT is matched with the average of five 2-min lidar data measurements corresponding to the same date and time period".

2. *What is meant by "average over different time periods": the 10 min period were named after the beginning of the period for the turbine and the end of the period for the lidars(or vice versa) and it could be fixed with a 10 min shift or the clocks were not synchronized during the campaign and you had to manually find the beginning of the 10 min period to be averaged?*

Thank you for this comment. We changed "time periods" for "time intervals" and included a clarifying parenthesis exemplifying the time intervals in which the lidar and SCADA averages measurements.

3. *How have you checked the time synchronization between the turbine and lidar signals?*

Yes, this is an important issue. We have added Figure 5 to demonstrate the synchronization between turbine and lidar signals using 80-m wind speeds.

4. *This section about time averaging and time synchronization should be moved before the "wind turbine" section since the time averaging and synchronization needed to be performed before producing the plots in figure 4.*

Thank you for this comment. However, plots in Figure 4 were obtained using nacelle-measured wind speed as recommended by St. Martin et al. (2016). We left this section last as it combines what is said in the previous two sections and it now includes synchronization between lidar and turbine measurements.

P8, l3-4 (and figure 5):

1. *How come the measure power is larger than for wind speed above 12m/s? this does not match with the blue dots in Figure 4a).*

Thank you for comparing these figures. However, measured power in Figure 4a also shows power above rated (measurements around 1.6 MW) for wind speeds between 11 and 14 m s^{-1}.

2. *For what range of wind speed shear, direction shear and TI was the power curve provided by the manufacturer? Could that explain the discrepancy between 5 and 8m/s?*

Thank you for noting this lack of information as these conditions have been previously found to alter a turbine's power curve. However, we were not able to obtain this information from the manufacturer. Still, we were not trying to find the cause for such discrepancies given that each of the four turbines

demonstrated differing power curves for different wind speed regimes. For instance, while turbine D showed overperformance for wind speeds between 9 and 10 m s^{-1}, turbine A showed slight underperformance. Therefore, given the observed discrepancies between each turbine's mean power curve and the manufacturer's, we chose to use our mean power curve for normalization to compare turbine operation changes compared to their average operation throughout the campaign. With mean power curve as baseline, if we normalize turbine power using the mean turbine operating conditions throughout the campaign, then shifts from this mean may be due to speed or direction shear.

P8, l7 to 11. I do not quite understand the point of the exercise with the Pearson correlation coefficient.

1. *What is the purpose of this comparison? Did you have some doubt about the lidar measurements accuracy? Has it been compared to another wind speed measurement (e.g. mast mounted anemometer or other lidar) before or after the campaign? Or is this to show somehow that there is a good correlation between the lidar wind speed and the turbine power, although it was placed rather far from the turbine(s)?*

The purpose of this comparison was to determine which wind speed data (nacelle anemometer or lidar) to use for each turbine's mean power curve. We used the Pearson correlation coefficient to find the power curve that resembled the most that of the manufacturer (see p.8, lines 16 – 20 on revised manuscript). However, we acknowledge that each turbine's mean power curve is different, and so we do not use the manufacturer's power curve as a reference frame.

2. *The nacelle anemometer measurements are expected to be disturbed by the rotor and the nacelle. The manufacturer power curve is provided with the free hub height wind speed on the x-axis. In order to get a comparable measured power curve using the nacelle wind speed, it must be corrected with a Nacelle Transfer Function (NTF)? Was this applied? If so, where did the NTF come from? If the nacelle wind speed was not corrected, it is to be expected that there is not be a good agreement with the manufacturer power curve.*

Thank you for your comment. We did not correct the power curve obtained using nacelle wind speed with a Nacelle Transfer Function. However, as stated above, the purpose of comparing power curves obtained using lidar- and nacelle-measured wind speed was to find the power curve that resembled the most that of the manufacturer so we could normalize observations in relation to each turbine's mean operating conditions. We clarified this in subsection 3.1, the updated manuscript for p.8, lines 16-17 reads as follows: "Consequently, mean power curves for each turbine were utilized as a reference value for normalization to have a consistent comparison of performance among individual devices."

p.9: "Directional shear": this section is hanging (missing numbering)

Thank you for catching this, we have added numbering for this subsection.

p9, lines 6 to 17: this should be in the introduction.

Thank you for this suggestion. We added the main idea of this paragraph to the introduction (p.2, lines 22 – 23).

P11, figure 7: there are average and median over the whole measurement period? Could you include a standard deviation or 25th, 75th percentile in the figure as well?

Thank you for this comment. We agree that it is very important to include the spread of the data in every plot, and so we tried this. However, adding this information obscures the main idea of this figure given that we have also added the evolution of speed shear into the same plot. Further, the purpose of these plots is to show the general evolution of shear, and correspondence between both shear parameters with time of day. For turbine performance, though, we included standard deviations.

P12, l.9: how does the LDWS and HDWS events correlate to wind speed shear and turbulence intensity?

Thank you for this helpful suggestion which has motivated a lot of analysis. A description of speed shear has been included in the updated manuscript. We included speed and direction shear relationships for similar wind speeds (Figure 13) and normalized performance segregated using both shear parameters (Figure 14). However, we did not have enough data to further segregate power production according to turbulence intensity.

Figure 10 to 13:

1. *are those results for Turbine D?*
2. *strong veer is expected to be correlated with strong speed shear – which is expected to have a large impact on the power performance. How do you know those results are not just due to the wind speed shear?*

Thank you for raising an interesting point. We have now included the effects of speed shear in our analysis and also considered the effect of direction shear for similar power law exponents (0.1 speed shear exponent bins). In the new Figures 15 and 16, we show the effects of direction shear for different wind speeds and 0.2 – 0.3, 0.3 – 0.4, and 0.4 – 0.5 speed shear exponents. We also included clarification in each figure's caption stating that results are for the four analyzed wind turbines.

p18, l.9 to p19, l3. The points you are trying to make with comparison to other studies need to be clarified. The reasons why you find them in contradiction with your own results are not clear.

Thank you for this suggestion. Though our analysis somewhat changed by taking speed shear into consideration, we tried to clarify the reasons for conflicting results with other studies. The most notable differing results correspond to the absence of underperformance for large veering observations recorded by Rareshide et al. (2009), and to asymmetries in the effects of wind veering and backing found by Wagner et al. (2010) and Walter et al. (2009).

Explanations to each diverging finding reads as follows; p.21, lines 23 – 26: "Conversely, Rareshide et al. (2009), looking exclusively at 8 m s^{-1} wind speeds, only reported underperformance for speed shear exponents around 0.2 and veering near 0.25 deg m^{-1}. Our results suggest more notable underperformance to occur for larger direction shear values, which were not considered in their study."; p.21, lines 31 – 34 and p. 22, lines 1 – 2: "Our dataset only evidenced statistically distinct power production between veering and backing for two speed shear ranges, suggesting the power asymmetries found by Walter et al. (2009) and Wagner et al. (2010) did not occur at these low shear conditions. Moreover, the small mean backing numerical values for these speed shear ranges indicate additional forcing mechanisms were in place for these underperformance observations. Not enough large backing observations were recorded to compare turbine performance against large veering atmospheric conditions."

P19, l15-17. This is often the challenge. But is no because the dataset is too small to bin them according to speed shear and direction shear (with statistical significance in al bins) that the effect of speed shear can be ignored. The speed shear or wind speed profile for this specific dataset has to be carefully

understood and described in the paper before drawing any conclusions on the effect of veer on the turbine power performance.

Thank you for this thoughtful suggestion. We included a complete characterization of speed shear in our manuscript (new figures 7-13) analyzing its evolution throughout the day, how it depends on wind speed, and its relationship with direction shear. We also included the combined effects of direction and speed wind shear on turbine performance (new figure 14), and isolated the effects of direction shear by considering specific power law exponent values (new figure 15).

P19, l21 to 33. I think it is outstretching to expand the discussion to skewed wake effect on power performance here (how do you make the different between the underperformance due to "standard "wake and skewed wake?) and is out of scope.

We agree that expanding the discussion to skewed wake effect on power performance may be out of scope, so we have deleted this paragraph.

Looking forward to reading you again. And thanks for giving me the chance to get back to this topic after many years.

Thank you very much for your thoughtful and insightful review – we greatly appreciate your insights.
Best regards, Miguel and Julie

Best regards, Rozenn

The effect of wind direction shear on turbine performance in a wind farm in central Iowa

Miguel Sanchez Gomez[1], Julie K. Lundquist[2,3]

[1]Department of Mechanical Engineering, University of Colorado Boulder, Boulder, 80303, United States
[2]Department of Atmospheric and Oceanic Sciences, University of Colorado Boulder, Boulder, 80303, United States
[3]National Renewable Energy Laboratory, Golden, 80401, United States

Correspondence to: Miguel Sanchez Gomez (misa5952@colorado.edu)

Abstract. Numerous studies have shown that atmospheric conditions affect wind turbine performance, however, some findings have exposed conflicting results for different locations and diverse analysis methodologies. In this study, we explore how the change in wind direction with height (direction wind shear), a site-differing factor between conflicting studies, and speed shear affect wind turbine performance. We utilized lidar and turbine data collected from the 2013 Crop Wind Energy eXperiment (CWEX) project between June and September in a wind farm in north-central Iowa. Wind direction and speed shear were found to follow a diurnal cycle, however they evolved differently with increasing wind speeds. Using a combination of speed and direction shear values, we found large direction and small speed shear to result in underperformance. We further analyzed the effects of wind veering on turbine performance for specific values of speed shear and found detrimental conditions in the order of 10% for wind speed regimes predominantly located in the middle of the power curve. Focusing on a time period of ramping electricity demand (0600 – 0900 LT) exposed the fact that large direction shear occurred during this time and undermined turbine performance by more than 10%. A predominance of clockwise direction shear (wind veering) cases compared to counterclockwise (wind backing) was also observed throughout the campaign. Moreover, large veering was found to have greater detrimental effects on turbine performance compared to small backing values. This study shows that changes in wind direction with height should be considered when analyzing turbine performance.

1 Introduction

Wind power generation directly depends on wind speed. Additionally, power depends on atmospheric conditions like static stability, shear and turbulence (e.g. Bardal et al., 2015; van den Berg, 2008; Kaiser et al., 2007; Rareshide et al., 2009; St. Martin et al., 2016; Sumner and Masson, 2006; Vanderwende and Lundquist, 2012; Wagner et al., 2010; Walter et al., 2009; Wharton and Lundquist, 2012). Idealized theories state that the power extracted by a wind turbine is a function of the blade element's efficiency (i.e. turbine blade design) and the available power flux through the disk swept by the blades (Burton et al., 2001). However, atmospheric turbine operating conditions diverge from simplified ones used for turbine design. Varying inflow speed and direction profiles, turbulence, transient conditions, and wake effects from upwind turbines alter power production.

Deleted: affects

Deleted: Directional wind

Deleted: was

Deleted: and to monotonically decrease

Deleted: different thresholds to distinguish between high-

Deleted: low-directional wind

Deleted: scenarios

Deleted: that larger thresholds evidence statistically-significant

Deleted: power production

Deleted: lower wind speeds. We further analyzed a threshold of 0.225 deg m^{-1}

Deleted: turbine underperformance

Deleted: below 8 m s^{-1}. Considering

Deleted: 0530

Deleted: occurs

Deleted: is undermining

Deleted: , however, future work on segregating speed and direction shear should be pursued to quantify the effects of only one factor on turbine power production.

Static stability in the lower planetary boundary layer is governed by temperature gradients that drive or suppress buoyancy (Stull, 1988). Three stability regimes are usually established; stable, neutral, and unstable conditions, corresponding to a stratified, equilibrated, and convective atmosphere, respectively. Several means of quantifying atmospheric stability have been employed in wind energy studies, including the dimensionless wind shear exponent (α), turbulence intensity, bulk Richardson number, and the Obukhov length. While some field measurements have provided insight into how stability affects power production, conflicting results have been reported in differing locations. At a wind farm identified only as "West Coast North America", Wharton and Lundquist (2012a,b) found an increase in wind turbine power production during stable atmospheric regimes. In contrast, at another site in the central plains of North America, the opposite effect occurred (Vanderwende and Lundquist, 2012). St. Martin et al. (2016) considered the effects of stability and turbulence at a test site near the Rocky Mountains in Colorado. They found stable conditions to enhance performance near rated speed, while undermining it for lower wind speeds. Their results regarding turbulence effects, however, agreed with theoretical findings by Kaiser et al. (2007) and with observations presented by Rareshide et al. (2009) that suggest a convective atmosphere decreases performance near rated wind speed and causes overperformance near cut-in wind speed.

Several factors could explain the difference in results between these stability regimes. First, the available data and thus the analysis method differs. Wharton and Lundquist (2012b) segregated power production regimes using wind shear exponents and turbulence intensity in a location with channeled flow. In contrast, Vanderwende and Lundquist (2012) employed the Richardson number and wind shear criteria to quantify local atmospheric stability on a wind farm that could experience directional wind shear. The conflicting results among studies suggest that either additional forcing mechanisms are present or that site-specific factors govern the effects on power production. One likely site-specific factor is the role of directional wind shear, which was not explicitly considered in the above studies but could differ between those sites.

Here we seek to resolve these conflicting results by quantifying the role of directional wind shear in turbine performance. Directional shear is the change of wind direction with height. The three main mechanisms for generating direction shear are the thermal wind, the inertial oscillation and surface stress. In the meteorological community, "wind veering" is used to describe the clockwise turning of the geostrophic wind with height, while "wind backing" describes the counter-clockwise turning of the geostrophic wind with height (Holton and Hakim, 2013). Veering tends to be associated with warm air advection, while backing is associated with cold air advection. Both these terms are associated with deep layers in the atmosphere rather than relatively shallow layers of the atmospheric boundary layer (ABL). Within the boundary layer, veering tends to be more common in the Northern Hemisphere due to the direction of the Coriolis force and the resulting Ekman layer.

In a wind energy context, directional shear causes the incoming wind to be misaligned with the rotor axis over some heights of the rotor swept area (Bardal et al., 2015) as the turbine tends to orient itself into the direction of the wind at hub height. Both veering and backing generate a substantial variation of the horizontal wind speed component orthogonal to the turbine axis altering the energy flux through the rotor and the turbine's capability to extract energy (Wagner et al., 2010). Veering decreases the mean relative wind speed experienced by a clockwise-rotating blade, while backing increases it (Wagner et al., 2010). In contrast, the opposite happens for the angle of attack. The angle of attack is larger for veering and smaller for backing

Deleted: channelled

Deleted: sought

Deleted: Both veering and backing generate a substantial variation of the horizontal wind speed component orthogonal to the turbine axis.…

(Wagner et al., 2010). Simulations by Wagner et al. (2010) also show that though backing increases both mean lift and drag over the blade, the resulting tangential force experienced by the rotor is reduced, while it is slightly augmented by veering. The increase in tangential force from wind veering results in a slight increase in power production, whilst wind backing slightly decreases power production.

The existing studies on the effects of atmospheric stability on power production differ in the role of directional wind shear. The Wharton and Lundquist (2012a,b) wind turbines, and St. Martin et al. (2016) testing site were surrounded by complex terrain that steered a channeled flow into the turbines and prevented the development of directional wind shear during stable conditions. In contrast, at the Vanderwende and Lundquist (2012) location, complex terrain did not prevent the occurrence of a changing wind direction with height.

Several methodologies have been employed for studying the effects of directional wind shear on turbine performance. Bardal et al. (2015) used measurements from a test site in the coastline of Norway without distinguishing between veering and backing. They found a small reduced power output below rated speeds for directional shear above 0.05 deg m^{-1}. Rareshide et al. (2009) found slight effects on turbine performance for large wind backing values using measurements from several sites across the Great Plains/Midwest region. Walter et al. (2009) characterized directional shear in Texas and Indiana, and used those findings to run blade-element simulations using the National Renewable Energy Laboratory (NREL) fatigue analysis structures and turbulence (FAST) model. Results from coupling power change simulations with observations evidenced potential power gains as large as 0.5% and losses as low as 3% when considering both speed and direction shear. Simulations by Wagner et al. (2010) employed a simplified model (HAWC2) finding slight increases in power production for veering and larger reductions from backing, for constant wind speed shear values.

In this present study, the effects of directional wind shear on power production were analyzed by separating the effects of speed shear using data collected in the 2013 Crop-Wind Energy eXperiment (CWEX-13) field campaign of a 150 MW onshore wind farm. Section 2 provides an overview of the dataset utilized for this study, which includes turbine power production and wind profiling lidar, and their respective filtering. Section 3 describes the definition of directional wind shear, speed shear and individual turbine's power curves. Wind shear characterization and its effects on turbine power production are summarized in sections 4 and 5.

Deleted: 2
Deleted: 3
Deleted: Directional
Deleted: outlined
Deleted: 4
Deleted: 5.

2 Data

2.1 Measurement site

The Crop Wind Energy eXperiment projects (CWEX) in 2010, 2011 and 2013 explored how wind turbines create changes in microclimates over crops (Rajewski et al., 2013, 2014, 2016), how the diurnal cycle affects wind turbine wakes (Lee and Lundquist, 2017; Rhodes and Lundquist, 2013), and how agricultural cropping and surface management impact wind energy production (Vanderwende and Lundquist, 2016). The 2013 campaign emphasized the impacts of atmospheric conditions like nocturnal low-level jets (Vanderwende et al., 2015) on wind turbine performance and the dynamics of wake variability (Bodini

Deleted: intended to quantify
Deleted: (Rajewski et al., 2013, 2014, 2016)

et al., 2017; Lundquist et al., 2014). These data have also been used to test approaches for coupling mesoscale and large-eddy simulation models (Muñoz-Esparza et al., 2017). The CWEX-13 field campaign took place between late June and early September 2013 in a wind farm in north-central Iowa. Measurements from several surface flux stations, a radiometer, three profiling lidars, and a scanning lidar were collected.

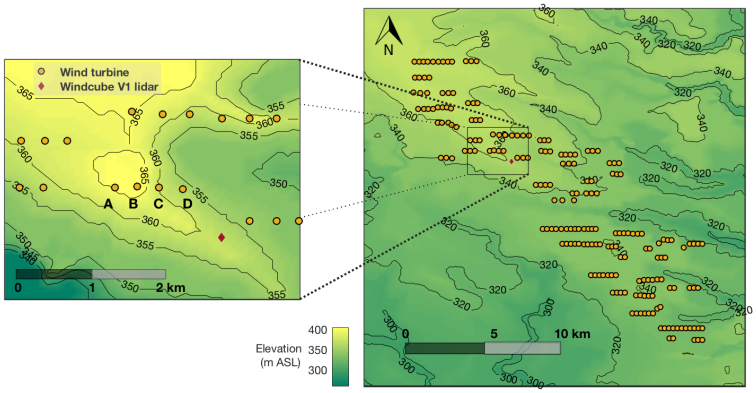

Figure 1. Schematic view of the wind farm in central Iowa where the CWEX-13 campaign took place. The turbines of interest for this study are marked as A, B, C and D.

The wind farm consisted of 200 wind turbines extending in a parallelogram with a long axis from the southeast to northwest (Figure 1). The northernmost 100 turbines were General Electric (GE) 1.5 MW extra-long extended (XLE) model and the southernmost 100 turbines were GE 1.5 MW super-long extended (SLE) model turbines. The land was generally flat with a slope smaller than 0.5 deg from southwest to northeast. Turbines were surrounded by a mixture of corn and soybeans, some wetland and lower terrain at the southern edge of the farm, and scattered farmsteads (Rajewski et al., 2013). The region of interest in the 2013 campaign comprised a subset of GE 1.5 MW XLE model turbines (see Table 1 for specifications). For this study, power production from four turbines near one Windcube V1 profiling lidar was utilized.

Table 1. Technical specifications of the turbines studied in the CWEX-13 field campaign (General Electric, 2009).

Rotor diameter (D)	82.5 m
Hub height	80 m
Rated power	1.5 MW
Cut-in wind speed	3.5 m s^{-1}
Rated power at	11.5 m s^{-1}
Cut-out wind speed	20 m s^{-1}

Deleted: The CWEX-13 field campaign took place between late June and early September 2013 in a wind farm in north-central Iowa. Measurements from several surface flux stations, a radiometer, three profiling lidars, and a scanning lidar were collected. These data have also been used to test approaches for coupling mesoscale and large-eddy simulation models (Muñoz-Esparza et al., 2017)

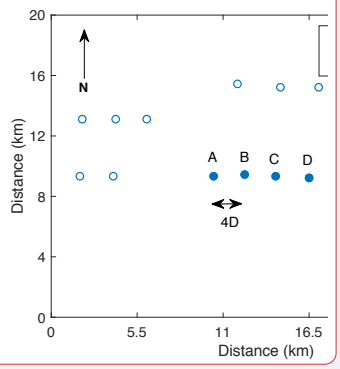

Deleted:

Deleted: diagram

Deleted: region

Deleted: consists

Deleted: .

Deleted: are

Deleted: are

Deleted: is

Deleted: are

Deleted: comprises

Deleted: (Figure 1).

2.2 Lidar

To quantify wind shear, we relied on data collected from the profiling lidar Windcube V1, designed by Leosphere, deployed during the CWEX-13 campaign. This Doppler wind lidar measured vertical profiles of speed and direction at nominally 1-Hz temporal resolution. It used a Doppler beam swinging (DBS) approach obtaining radial wind measurements along four cardinal directions at an inclination of 62.5º above the horizon (Vanderwende et al., 2015). The components of the flow were then calculated from the four separate line-of-sight velocities (Lundquist et al., 2015). The CWEX-13 campaign collected wind measurements from 40 to 220 m above ground level at 20-m increments. This study focuses on 2-min average measurements from 40 to 120 m, which comprise the entire turbine rotor layer.

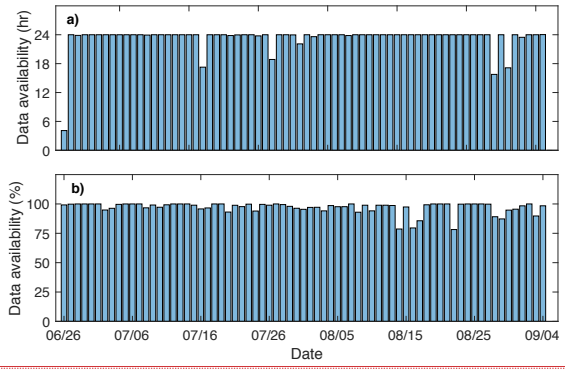

Figure 2. Lidar (a), and turbine (b) data availability for the duration of the campaign. Turbine power availability only corresponds to percentage of power measurements recorded for wind speeds above 2.5 m s^{-1}.

Wind lidar data was available throughout the campaign (Figure 2a). 2-min wind speed (80 m height) observations for each day only presented significant shortages (>30% of day) for June 27 and August 28. Similarly, power mean data availability for the four analyzed wind turbines and wind speeds above 2.5 m s^{-1} presented great uniformity, having largest shortages (>20%) for August 14, 16 and 22, and an average 30-min availability of 92%.

The prevailing wind direction for the recorded period in this wind plant was primarily south-southwesterly having a mean wind speed of 8.21 m s^{-1}. However, 21% of wind had a strong northerly component (Figure 3), generally associated with frontal passages. The infrequent easterly and westerly winds (90±10 deg and 270±10 deg) were discarded to ensure the turbines were not experiencing wakes from their nearby (within 5 rotor diameters *D*) neighbors. Previous studies in this wind farm have found wakes in stable conditions to persist for long distances (up to 17.5 *D*) downwind (Bodini et al., 2017), and so therefore all winds with northerly components were also discarded to ensure the profiling lidar was not affected by wakes. Further, only wind speeds between cut-in (3.5 m s^{-1}) and cut-out (20 m s^{-1}) were considered.

Deleted: directional
Deleted: rely
Deleted: measures
Deleted: uses
Deleted: are
Deleted:
Deleted:
Deleted: is
Deleted:),
Deleted: having
Deleted: Likewise, turbine
Deleted: has

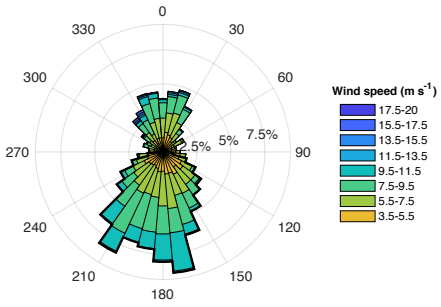

Figure 3. Wind rose for lidar hub-height altitude (80-m) measured wind speeds between cut-in and cut-out. The black outline highlights the wind direction sector (southerly) used for subsequent data analysis.

The remaining analysis only considers winds with southerly components (wind direction between 100 and 260 deg), and speeds between 3.5 and 20 m s^{-1}. Of note, most winds above 11 m s^{-1} occurred with the northerly frontal passages, so this direction filtering also effectively restricts the analysis to wind speeds below 11 m s^{-1}.

2.3 Wind turbines

The subset of turbines employed for this study consists of four clockwise-rotating (while looking downwind) GE XLE 1.5-MW, variable blade pitch wind turbines (see Table 1 for specifications). Power production, nacelle wind speed and blade pitch angles were provided by the wind farm operator as 10-min averages recorded via the supervisory control and data acquisition (SCADA) system of each turbine. To analyze how wind shear impacts power production, turbine underperformance during curtailments was filtered following the blade pitch angle approach of St. Martin et al. (2016). Blade pitch angles are controlled to maximize power production as a function of nacelle-measured wind speed, and large blade pitch angles typically represent curtailed conditions or rapidly changing conditions. Therefore, we discarded 10-min periods with blade pitch angles outside ±4.5 the mean absolute deviation (MAD) for each 0.5 m s^{-1} wind speed bins (Figure 4).

Deleted: directional

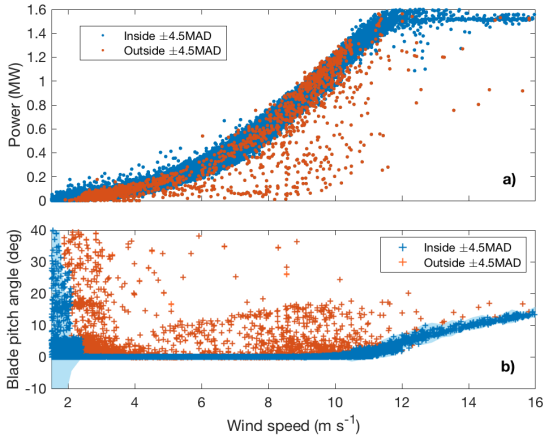

Figure 4. Power curve based on nacelle-measured wind speed (a), and blade pitch angle from a single blade (b) combining data from the four analyzed wind turbines. Red scatter points show 10-min periods filtered out for curtailments, represented by data points outside the MAD envelope. The blue envelope in bottom graph represents ±4.5 MAD of the blade pitch angle within 0.5 m s^{-1} wind speed bins.

Deleted:).

Deleted: Blue

Deleted: ms

2.4 Time averaging

Turbine- and lidar-recorded data are averaged over different time intervals by their respective data-acquisition systems (2-min for lidar, and 10-min for turbine). Matching turbine performance with atmospheric conditions was performed by averaging 2-min lidar measurements for the corresponding 10-min turbine power production period. For example, turbine data for July 04, 2013 from 0500 to 0510 LT is matched with the average of five 2-min lidar data measurements corresponding to the same date and time period. As is illustrated in Figure 5, turbine and lidar data were synchronized for the duration of the campaign.

Deleted: periods.

Deleted: -

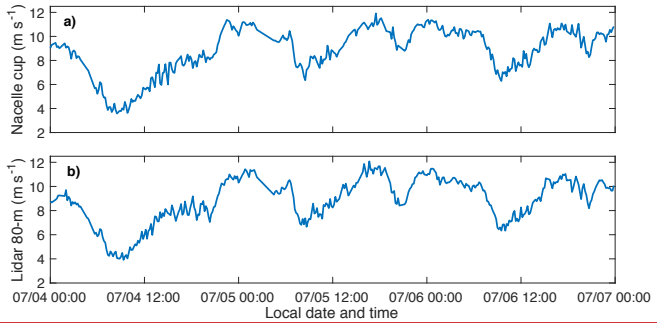

Figure 5. Time series from 00:00 July 04, 2013 to 00:00 July 07, 2013 of hub-height wind speeds measured by the cup anemometer on the nacelle of Turbine A (a), and 80-m wind speeds measured by the lidar (b).

3 Methods

3.1 Turbine power curves

According to the International Electrotechnical Commission's Wind Turbine Power Performance Standard (2005), wind turbine power performance characteristics are determined both by the measured power curve and the annual energy production. The measured power curve is obtained by simultaneously collecting data from meteorological variables and turbine performance over long periods of time. Wind speed is measured at hub height using cup anemometers mounted on a meteorological mast positioned 2 – 4 rotor diameters upwind of the turbine, and power output is recorded using a power measurement device (e.g. power transducer) between the wind turbine and the electrical connection. Measurements are averaged over 10-min time periods. A database for a wide range of wind speeds (0.5 m s^{-1} bins) is used to establish the relationship between the nacelle-height wind speed and wind turbine power output. General Electric's power curve for the 1.5 MW wind turbines in this study is shown in Figure 6 as the dashed line.

Power production for the duration of this campaign reflected persistent differences from the manufacturer's reference values at wind speeds below 8 m s^{-1} and above rated (e.g. Turbine C in Figure 6). Consequently, mean power curves for each turbine were utilized as a reference value for normalization to have a consistent comparison of performance among individual devices. Turbine power curves using nacelle-measured wind speed, and lidar-measured wind speed filtering easterly, westerly and northerly winds were compared. The Pearson correlation coefficient was used in each case to determine which power curve showed highest correspondence to the manufacturer's power curve for wind speeds below rated. Power curves obtained using lidar-measured wind speed displayed higher resemblance to GE curves (average $\rho = 0.9590, p = 0.00$) than power

Deleted: (

Deleted: normalized

curves obtained from nacelle-measured wind speed (average $\rho = 0.9061$, $p = 0.00$). Therefore, normalization was performed with respect to each turbine mean power curve obtained using lidar-measured wind speed.

As suggested by the histogram in Figure 6, the frequency of occurrence changed with wind speed, roughly following a Weibull distribution with a shape factor of 2.05 and a 6.9 m s^{-1} scale parameter. To determine if the sample size (number of power observations) for each 0.5 m s^{-1} wind speed bin was large enough for estimating each turbine's population mean (observed power curve), we calculated the required sample size to have a 99.5% confidence that the error (e) in the observed mean power does not exceed half the difference of mean power between two adjacent wind speeds. The power estimator ($\hat{p}$) is assumed to be a normally distributed estimator of the real turbine power (p) for each wind speed bin, then their difference is a normal distribution (Walpole, 2007):

$$\frac{\hat{p}-p}{\sqrt{Var(\hat{p})}} \sim N(0,1) \quad (1)$$

The allowable error was designated as half the difference in mean power between two adjacent wind speeds ($e_V = 0.5\,(\hat{p}_{V+0.5} - \hat{p}_V)$), and so the probability of the real and observed mean difference being greater than the allowable error ($P_{(|\hat{p}_V - p_V| > e_V)}$) is 0.005 (i.e. 99.5% confidence). A property of a normal distribution is that this same probability holds for $|\hat{p}_V - p_V| > z_{\alpha/2}\,\sigma_V/\sqrt{n}_V$. Thus, the minimum sample size to have 99.5% confidence that the error in the observed mean power does not exceed half the difference of mean power between two adjacent wind speeds is $n_V = z_{\alpha/2}\,\sigma_V\sqrt{/e_V}$. Every turbine had sufficient data points for wind speeds between 4 and 11 m s^{-1} (referred to as the partial load regime), and every 0.5 m s^{-1} bin within this range had at least 106 observations, supporting the assumption for a normally distributed estimator.

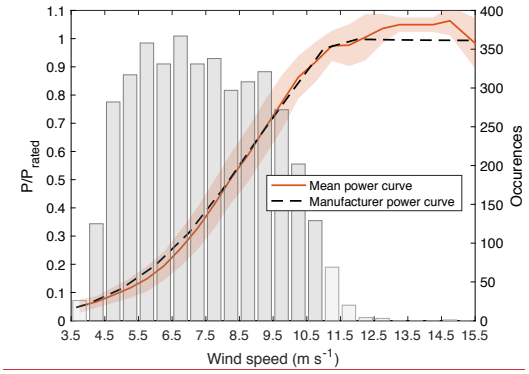

Figure 6. Mean power curve for Turbine C based on 80-m lidar wind speed measurements overlayed over the number of power production cases for each 0.5 m s^{-1} wind speed bins. The shaded region in the power curve corresponds to ±1 standard deviation, and the dark grey histogram corresponds to the wind speed ranges considered in this study.

Deleted: Figure 5,
Deleted: changes
Deleted: 4.1
Deleted: factor or 8.2.
Deleted: ,→
Deleted: 01

3.2 Wind shear

Directional wind shear is defined as the change in wind direction with height, and speed shear corresponds to the change in the mean horizontal wind speed. One mechanism for generating wind shear is the vertical shear of geostrophic wind referred to as thermal wind. The thermal wind is caused by large-scale horizontal temperature gradients that can be created by sloping terrain, fronts, land-sea interfaces, and large-weather patterns (Stull, 1988). Wind shear overnight is also generated by the inertial oscillation (Blackadar, 1957; Van de Wiel et al., 2010). The inertial oscillation is the rotation in the wind vector in the residual layer caused by a force imbalance at sunset, when mixed layer turbulence ceases. As frictional stress diminishes after sunset, pressure gradients tend to accelerate subgeostrophic winds in the mixed layer back toward geostrophic. Inertia from the counteracting Coriolis force induces an oscillation in the wind vector causing it to become supergeostrophic and to turn clockwise (northern hemisphere) with time (Stull, 1988). A third forcing mechanism is frictional drag with the ground. Turbulent momentum fluxes in the boundary layer reduce the actual wind speed near the surface. The Coriolis force, being directly proportional to the wind speed, decreases creating a force imbalance with the pressure gradients. As a result, the actual surface wind vector is directed across the isobars toward low pressure (Holton and Hakim, 2013).

Directional shear in this study is calculated as the shortest rotational path between wind vectors at 40 and 120 m above ground level, normalized over vertical distance between the measurements. For example, a case with southerly winds at 40 m and westerly winds at 120 m would be calculated as 90 deg shear over the 80 m layer depth, or 1.125 deg m^{-1}. We characterize speed shear through the dimensionless wind shear exponent α using the power law expression,

$$V = V_R \left(\frac{z}{z_R}\right)^{\alpha}, \quad (2)$$

where V is the mean horizontal wind speed at height $z = 120$ m, and V_R is the mean horizontal wind speed at reference height $z_R = 40$ m above ground level.

Speed and direction wind shear alter the available power of the air through the turbine and its ability to extract energy from the wind (Wagner et al., 2010). The available power in the air flowing across a disc is proportional to the projection of the velocity vector over the disc area,

$$P_{avail.} \propto \left(\vec{V} \cdot \vec{n}\right)^3, \quad (3)$$

where $\vec{V}$ is the wind vector, $\vec{n}$ is the unit vector normal to the disc area, and P_{avail} is the available power in the air. Several models have shown that speed shear exponents above 0 and below 0.33 result in lower available power over the whole rotor area, whereas larger α values increase the energy flux compared to a uniform flow with hub-height speed (e.g. Antoniou et al., 2009; Bardal et al., 2015). Blade aerodynamic performance with shear also diverges from design conditions. Changing wind direction and speed with height makes the relative velocity between the air and the blades, and the effective angle of attack to vary (Wagner et al., 2010), causing the turbine blades operate at suboptimal blade pitch angles.

The literature includes a range of different classification thresholds to analyze contrast high wind shear and low wind shear to explore its effects on turbine performance. Bardal et al. (2015) utilized a threshold of 5 deg over a vertical extent of 100.6

Deleted: Directional wind

Deleted: .

Deleted: directional

Deleted: the absolute value of

Deleted: directional

Deleted: (HDWS)

Deleted: directional

Deleted: (LDWS)

m (or 0.0497 deg m^{-1}) to distinguish between high and low direction shear scenarios in a wind farm on the coastline of mid-Norway. They found small detrimental effects of high veering on power production for wind speeds near 7, 8 and 9.5 m s^{-1} (Bardal et al., 2015). To examine the effects of speed shear, they considered different ranges of the power law exponent and found a reduction of turbine efficiency for high-shear ($\alpha > 0.15$) conditions in the partial load regime (Bardal et al., 2015). Rareshide et al. (2009) considered a statistical description specific to several sites across the Great Plains/Midwest region, encountering slight performance reductions for wind backing of -0.25 deg m^{-1} and near uniform speed profiles. Walter et al. (2009) performed blade-element modeling using the fatigue analysis structures and turbulence model (FAST) from the National Renewable Energy Laboratory to quantify the effects of speed and direction shear on performance. Simulation results for 8 and 10 m s^{-1} wind speeds showed a maximum instantaneous 6% underperformance occurring for wind speed shear exponents of 0.35 and wind backing of -0.472 deg m^{-1}. Here, we considered the combined effect of direction and speed shear on normalized turbine performance to define the shear values that segregate under- and overperformance in this wind farm.

Deleted: HDWS

Deleted: LDWS

Deleted: HDWS

Deleted: different thresholds

Deleted: HDWS scenarios

Deleted: order to identify power production differences compared to LDWS cases. HDWS scenarios for the 10-min power production periods where defined as those having the 10-min mean directional

Deleted: shear above the selected threshold, or having more 2-min HDWS than LDWS cases

4 Results

4.1 Wind shear characterization

Deleted: Directional wind

A predominance of wind veering was observed in this site compared to wind backing cases (Figure 7a). Wind veering occurred more than 77% of the time and displayed larger numerical mean and maximum values (0.0939 deg m^{-1} and 1.83 deg m^{-1}, respectively) compared to backing (-0.0144 deg m^{-1} and -1.17 deg m^{-1}, respectively).

Deleted: Figure 6

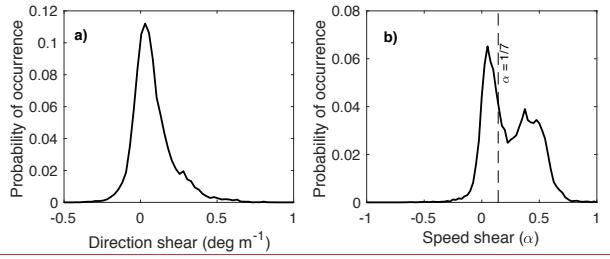

Figure 7. Probability distribution for direction shear (a), and speed shear (b) in the rotor layer (40 – 120 m above ground level).

The speed shear probability distribution was bimodal, with a narrow peak centered around 0 and a broad peak close to 0.4 (Figure 7b). An increase of speed with height was observed 88.6% of the time, from which 53% was above 0.225. Further, 60% of the recorded data lays above the commonly used 1/7 power law exponent.

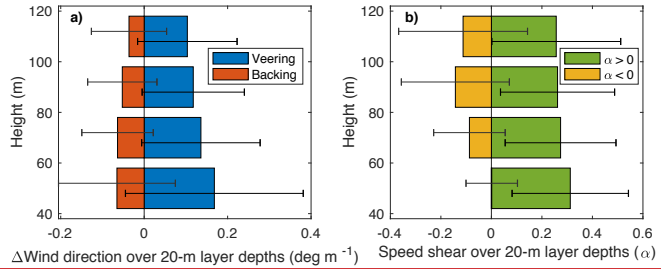

Figure 8. Wind direction (a), and speed shear (b) evolution with height across the rotor layer.

Both direction and speed shear had a tendency to decrease with height. Figure 8a illustrates how wind direction evolved differently through the rotor layer for veering and backing cases. Both clockwise and counterclockwise wind direction rate of change were larger in the lower rotor layer. Directional shear was 1.6 times larger from 40 to 60 m compared to 100 to 120 m above ground level for veering, and 1.79 times larger for backing. When considering the absolute value of the wind vector rotation, the lower layer (40 to 60 m) experienced an average change in wind direction 1.55 times larger than the upper layer (100 to 120 m). Figure 8b demonstrates how wind speed changed unevenly for positive and negative power law exponents. Negative power law exponent cases only started evidencing decreasing wind speeds with height above 60 m, whereas positive α values presented the largest rate of change in the lower rotor layer. Speed shear was 1.2 times larger from 40 to 60 m compared to 100 to 120 m above ground level for positive shear values.

Direction **and** speed shear at the test site varied accordingly with time of day (Figure 9). The correlation between both parameters is 0.9. Nighttime cases showed an evolving surface layer that does not reach equilibrium, as is depicted by consistently increasing directional shear across the rotor layer at an average rate of 0.0304 deg m^{-1} hr^{-1}, and 0.0117 h^{-1} for speed shear from before sunset until just after sunrise. Daytime cases, on the other hand, experienced a rapid morning transition following sunrise (-0.1171 deg m^{-1} of directional shear, and -0.0723 of speed shear per hour) followed by a fairly consistent surface layer having a slowly decreasing mean directional shear of 0.004 deg m^{-1} per hour (0.0082 increase of α per hour). Average changes in wind direction (speed) with height at night was 2.6 (4.2) times larger than during daytime after the morning transition period.

Deleted: evolves

Deleted: is

Deleted: is

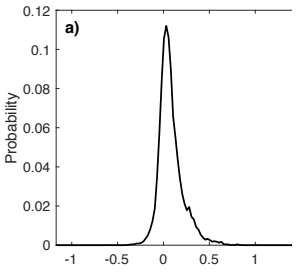

Deleted:
Figure 6. Probability distribution for direction shear (a),

Deleted: wind direction evolution (b) in the rotor layer (40 – 120 m above ground level).¶
Directional wind

Deleted: Figure 7).

Deleted: .

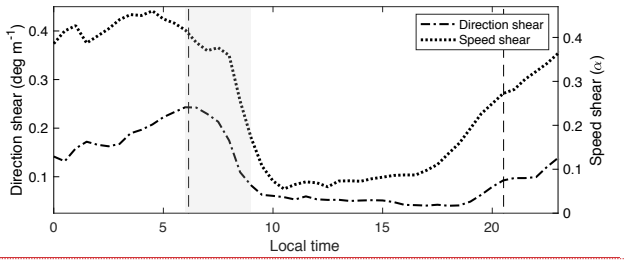

Figure 9. Diurnal cycle of mean wind direction and speed shear for wind speeds between cut-in and cut-out. Dashed vertical lines indicate sunrise and sunset times for August 1, 2013, the mid-point of the dataset analyzed here. The grey shaded region indicates the morning transition period (0600 – 0900 LT).

Of particular interest is the morning time period (from 0600 to 0900 local time) which, according to the U.S. Energy Information Administration (2019), experiences increasing electricity demand in the Midwest region. Wind shear presented its largest rate of change during this time period (Figure 9). At this time, nearly 50% of the recorded data between cut-in and cut-out wind speed was within 5 and 8 m s^{-1}, with a mean direction and speed shear of 0.196 deg m^{-1} and 0.37, respectively. This average shear exceeded the mean daytime (0.0838 deg m^{-1}, 0.168) and whole-day (0.1137 deg m^{-1}, 0.258) values, and nighttime (0.1613 deg m^{-1}, 0.39) direction shear value.

Though speed and direction shear varied proportionally throughout the day, they had opposite monotonical relationships with wind speed. As wind speed increased, so did speed shear, but direction shear decreased (Figure 10). Directional shear declined with increasing wind speed for both daytime and nighttime cases. While directional shear at night was generally larger than during the day, in both cases direction shear decreased at a median rate of around 0.0166 deg m^{-1} for each increase in m s^{-1} in wind speed. The power law exponent increased proportionally with wind speed at a rate of 0.0672 during nighttime for speeds below 9 m s^{-1}, and then stabilized. During daytime, a growth of 0.0184 in α occurred for each increase in m s^{-1} in wind speed up to 7.5 m s^{-1}; for higher speeds, speed shear decreased at a rate of -0.0195 for each increase in m s^{-1}. Daytime is defined as the period between sunrise as sunset for each date, and nighttime corresponds to the complementary period. Daily sunrise and sunset information were estimated using NOAA's sunrise/sunset calculator (National Oceanic and Atmospheric Administration, 2019). Median values appear in Figure 10 rather than mean values as the data presented a large spread with a large percentage of outliers. Outliers are considered observations outside the quantile 3 (75th percentile range) plus or minus a predetermined interquartile range (range between 25th and 75th percentile) for each 0.5 m s^{-1} wind speed bins (Q3±1.5IQ).

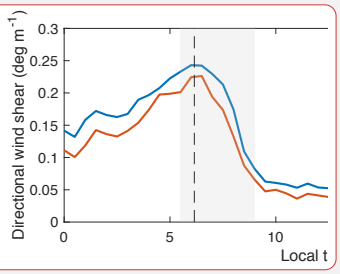

Deleted:

Deleted: directional

Deleted: 0530

Deleted: As directional

Deleted: it also

Deleted: an inverse

Deleted: relationship with wind speed.

Deleted: decreased

Deleted: (Figure 8).

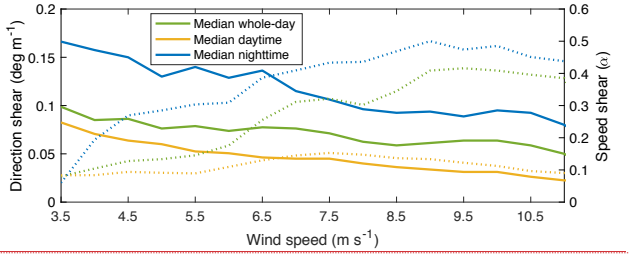

Figure 10. Direction (solid line) and speed (dotted line) wind shear variation with 80-m wind speed using each day's sunrise/sunset times of day.

Nighttime shear exceeded that during the day for wind speeds between cut-in and rated speed (Figure 10). Median nighttime directional wind shear was at least 1.8 times as large as daytime cases for wind speeds between cut-in and rated speed. The highest percentage difference occurred near rated wind speeds, where nighttime directional shear was 3.5 times larger than that during the day. Median speed shear during the night was on average 3.2 times larger than during daytime and presented the largest differences near rated speeds (about 4 times larger for wind speeds between 8 and 11 m s^{-1}).

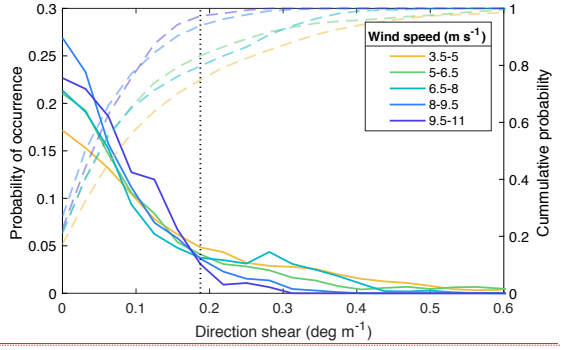

Figure 11. Directional wind shear probability density (solid lines) and cummulative (dashed lines) distributions for 1.5 m s^{-1} wind speed regimes. The black dotted line marks 0.1875 deg m^{-1} of directional wind shear.

Large directional wind shear tended to occur at wind speeds below 8 m s^{-1} (Figure 11). The number of occurrences of directional wind shear cases above 0.1875 deg m^{-1} in this site varied considerably for wind speeds above and below 8 m s^{-1}. The number of observed cases of directional shear larger than 0.1875 deg m^{-1} followed a similar trend for wind speeds between cut-in and 8 m s^{-1}, accounting for approximately 20% of observations. Conversely, wind speeds between 8 m s^{-1} and rated

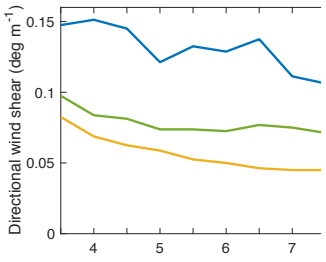

Deleted:

Deleted: . Directional

Deleted: (Figure 8).

Deleted: occurs

Deleted: is

Deleted: Of particular interest is the morning time period (from 0530 to 0900 local time) which, according to the U.S. Energy Information Administration (2019), experiences increasing electricity demand. Directional wind shear presented its largest rate of change during this time period (Figure 7). At this time, nearly 60% of the recorded data between cut-in and cut-out wind speed was within 4 and 8 m s^{-1} with a mean directional shear of 0.2257 deg m^{-1}. This average directional shear exceeds the mean daytime (0.0838 deg m^{-1}), whole-day (0.1137 deg m^{-1}), and nighttime (0.1613 deg m^{-1}) values.¶

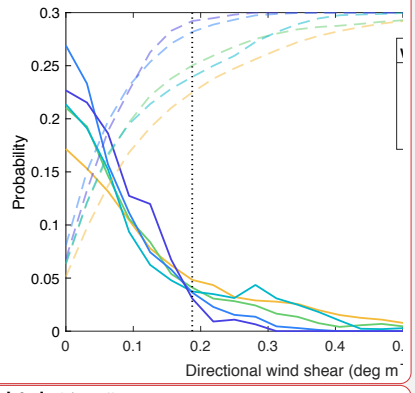

Deleted: (Figure 9).

Deleted: follows

Deleted: 80

speed reported considerably fewer cases above 0.1875 deg m^{-1} of directional shear (~4% of observations for each 1.5 m s^{-1} wind speed bin).

Deleted: report

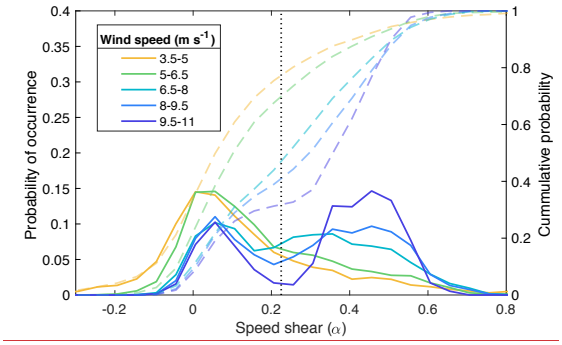

Figure 12. Speed shear probability density (solid lines) and cummulative (dashed lines) distributions for 1.5 m s^{-1} wind speed regimes. The black dotted line marks $\alpha = 0.225$.

Moved (insertion) [1]

Speed shear distributions changed dramatically for wind speeds above and below 6.5 m s^{-1} (Figure 12). Wind speeds near cut-in depicted a single peak centered at zero-shear with a broad right tail. Above 6.5 m s^{-1} wind speeds, power law exponent density distributions were bimodal, where increasing speeds displayed a trend for more cases of large shear values. Cumulative probability distributions for moderate and large wind speeds (> 6.5 m s^{-1}) displayed a curvature change from concave to convex around $\alpha = 0.225$. More than 70% of observations occurred at speed shear values below 0.225 for wind speeds between cut-in and 6.5 m s^{-1}. In contrast, only 32% of the recorded data presented shear values below 0.225 for wind speeds above 9.5 m s^{-1}, and less than 50% for 6.5 – 9.5 m s^{-1} wind speeds.

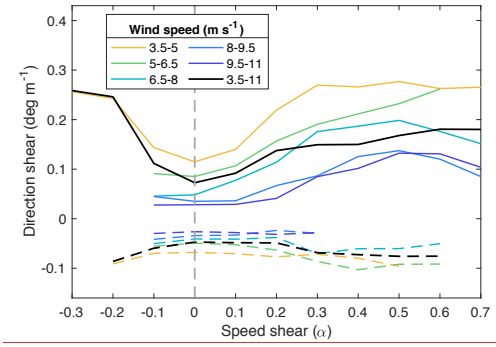

Figure 13. Mean speed and direction shear relationship for similar hub-height wind speed regimes (1.5 m s^{-1} bins). Solid lines correspond to wind veering and dashed lines to wind backing. Black lines correspond to the mean for all wind speeds. The dashed grey line marks zero-speed shear value.

Moved (insertion) [2]

Both shear parameters were correlated for similar hub-height wind speed regimes (Figure 13). The correlation coefficient for increasing speed and direction shear values (veering and backing) is 0.9, and for decreasing direction and increasing speed shear (veering and backing) is -0.9. The largest rate of change of shear parameters occurred for negative α values, where direction shear increased at an average rate of 0.735 deg m^{-1} (0.607 deg m^{-1}) per unit decrease (increase) of speed shear for veering (backing). Positive power law exponents displayed a small mean rate of change per unit increase of speed shear for veering and backing (0.165 deg m^{-1} and 0.063 deg m^{-1}, respectively). Further, smaller wind speeds evidenced a stronger relationship between speed and direction shear. Mean veering increased at an average rate of 0.347 deg m^{-1} per unit increase of speed shear for wind speeds below 8 m s^{-1} ($0 \leq \alpha \leq 0.4$), whereas veering increased at a rate of 0.21 deg m^{-1} for speeds above 8 m s^{-1}. Mean backing displayed an additional dissimilarity for $0 \leq \alpha \leq 0.4$, where a positive correlation existed near-rated speeds (>8 m s^{-1}), and a negative one for lower wind speeds (0.04189 deg m^{-1} and -0.0709 deg m^{-1} per unit increase in α, respectively).

4.2 Effects on turbine performance

Segregating normalized turbine power into speed shear (α) and direction shear (β) combinations revealed a threshold (referred to as α/β threshold from now on) that separates over- and underperformance at this wind farm (Figure 14). Speed and direction shear combinations that satisfy Eq. (4) tended to result in turbine performance equal to the mean observed throughout the campaign:

$$\beta = \frac{2}{3}\alpha - 0.1 \quad (4)$$

Turbine performance for atmospheric conditions that lay above the α/β threshold in Figure 14 resulted in underperformance for this dataset. Mean normalized power above and below the threshold was 0.94 and 1.01, respectively. Furthermore, this threshold allowed to distinguish power production in a statistically significant way (99.99% significance) for above- and below-threshold cases. A multiway analysis of variance revealed that both speed and direction shear affect the mean of normalized turbine performance (turbines A, B, C and D) for observations above and below the α/β threshold. Individual turbines' normalized performance evidenced similar results as combining the altogether (not shown). Every analyzed turbine displayed significant differences for normalized turbine power for cases above and below the threshold (99.99% significance).

Small wind backing and small veering showed similar effects on turbine performance (Figure 14). Veering below 0.1 deg m^{-1} and backing above -0.1 deg m^{-1} only reported statistically distinct (1% significance) normalized performance for speed shear exponents between 0.3 – 0.4 and 0.5 – 0.6. Clockwise direction shear resulted in slight overperformance (1.00 and 1.06 for $0.3 < \alpha < 0.4$ and $0.5 < \alpha < 0.6$, respectively). In contrast, counterclockwise direction shear resulted in underperformance (0.90 and 0.97 for $0.3 < \alpha < 0.4$ and $0.5 < \alpha < 0.6$, respectively). Mean negative direction shear was near-zero for both speed shear ranges (-0.036 deg m^{-1} for $0.3 < \alpha < 0.4$, and -0.035 deg m^{-1} for $0.5 < \alpha < 0.6$). Further, mean normalized turbine power production was 0.9806 for all backing observations throughout the campaign. Veering observations displayed similar results as mean normalized performance was 0.9877. Atmospheric conditions for all wind veering observations were predominantly just above the α/β threshold. Mean direction and speed wind shear were 0.118 deg m^{-1} and $\alpha = 0.31$, respectively. Wind backing cases were generally below the α/β threshold ($\alpha = 0.12; \beta = -0.031\ \mathrm{deg\ m^{-1}}$).

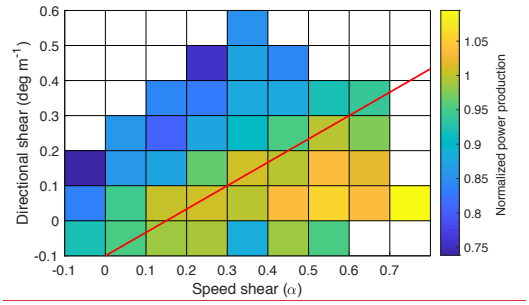

Figure 14. Mean normalized power production (turbines A, B, C and D) for all combinations of speed and direction shear that present more than 30 observations. The red line represents the α/β threshold.

Because one of the main differences between the Wharton and Lundquist (2012b) and Vanderwende and Lundquist (2012) studies was the occurrence of directional wind shear at the different sites, we here examined the effect of the shear of wind direction on turbine performance. To separate the effect of speed shear from that of direction shear, we isolated turbine performance that transpired within a 0.1 power law exponent interval and segregated observations using the α/β threshold for

Deleted: We tested a range of threshold values of directional shear to distinguish HDWS and LDWS scenarios. Figure 10 illustrates the normalized difference in power output between high- and low-shear scenarios defined by different thresholds for different wind speed regimes

each speed shear bin. **Figure** 15 illustrates how turbine performance was undermined with larger directional wind shear for different wind speed regimes. Mean normalized power was statistically distinct (1% significance) for wind speeds between 5.5 – 6 m s^{-1} and 7.5 – 8 m s^{-1}, and speed shear ranges (0.1 bins) between 0.2 and 0.4. Moreover, turbine performance differed (99% confidence) for 5.5 – 9 m s^{-1} wind speed regimes when considering power law exponents between 0.2 and 0.3 (**Figure** 15a). Normalized mean turbine performance for these wind speed regimes was 1.03 and 0.85 for cases below and above the threshold, respectively. Larger speed shear (**Figure** 15b) presented additional differences for smaller and larger wind speeds (4 – 4.5 m s^{-1}, 9 – 10 m s^{-1} and 11 – 11.5 m s^{-1}), however speeds in the middle of the partial load regime did not present as many significant differences (1% significance). Normalized mean turbine performance was 1.02 and 0.90 for statistically distinct wind speed regimes below and above the threshold, respectively.

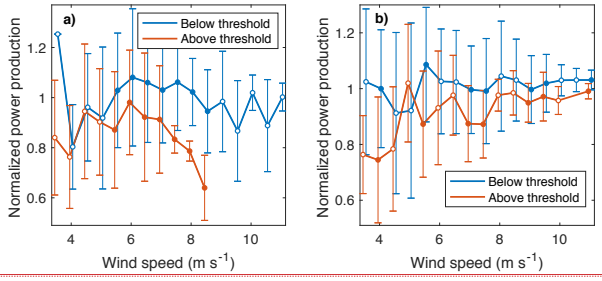

Figure **15**. Mean normalized power production (**turbines A, B, C and D) of observations above and below the α/β threshold for speed shear between 0.2 – 0.3 (a), and 0.4 – 0.5 (b). Filled circles are statistically distinct. Errorbars** represent 1 **standard deviation from the mean.**

Power variability can exert significant impact during morning hours, when power demand tends to increase. Throughout all power production periods, from 0600 to 0900 local time, 47.6% of the dataset reported speed and direction shear combinations above the α/β threshold. Further, normalized performance for $0.3 < \alpha < 0.4$, the power law exponent bin that presented the greatest number of observations above the threshold just after sunrise, depicted statistically distinct (1% significance) values for wind speed regimes between 5 – 6.5 m s^{-1}, 7.5 – 9 m s^{-1} and 10 – 10.5 m s^{-1} for above- and below-threshold cases (Figure 16). Normalized mean turbine performance for these wind speed regimes was 1.08 and 0.87 for cases below and above the threshold, respectively.

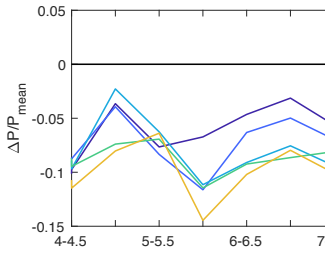

Deleted:

Deleted: **differences for high and low directional wind shear scenarios defined using different thresholds based on lidar 80-m height wind speed.**¶
As larger HDWS thresholds were considered, the effect on power production starts to be reflected at lower wind speeds (Figure 10). Thresholds below 0.1 deg m^{-1} failed to distinguish power production ... [1]

Deleted: are not shown). Using a

Deleted: of 0.1 deg m^{-1}, none of the four individual turbines agreed on a 0.5 m s^{-1} wind speed regime in which they had different medians with 5% significance for high and low directional shear cases. ... [2]

Deleted: 7.5 and 8 m s^{-1}. A 0.15 deg m^{-1} directional shear limit only resulted in one 0.5 m s^{-1} wind speed range (7.5 – 8 m s^{-1}) where individual turbines agreed in both the median and mean differences ... [3]

Deleted: deg m^{-1} exposed more dissimilarities between high and low directional wind shear scenarios. Mean and median differences for individual turbines and their combined normalized power production matched for wind speeds between 7 and 8 m s^{-1} (5% ... [4]

Deleted: **absolute deviation from the median. Only 0.5 m s^{-1} wind speed bins with more than 30 data points are plotted.**¶
For a threshold of 0.225 deg m^{-1}, the effects of HDWS on combined-turbine power production were most significant for wind speeds ... [5]

Deleted:) for HDWS scenarios compared to LDWS cases for the formerly mentioned wind speed regimes. Combined median normalized power revealed significantly affected (5% significance) performance for HDWS scenarios for 4 – 8 m s^{-1}. Median ... [6]

Moved up [1]: Figure 12.

Deleted: **Mean normalized power production for high and low wind veering and backing scenarios defined using a threshold of ±0.225 deg m^{-1}. Error bars represent 1 standard deviation. Only** ... [7]

Moved up [2]: **Figure 13.**

Deleted: **Normalized power production for high and low directional wind shear scenarios defined using a threshold of 0.225 deg m^{-1} from 0530 to 0900 local time. Black lines correspond to median values and grey ones to mean values. Error** ... [8]

Deleted: 0530 to 0900 local time, the averaged directional wind shear was 0.2064 deg m^{-1} for wind speeds between 4 and 10.5 m s^{-1}. Combined-turbines mean and median normalized power production were significantly (99% confidence for the means and 95% ... [9]

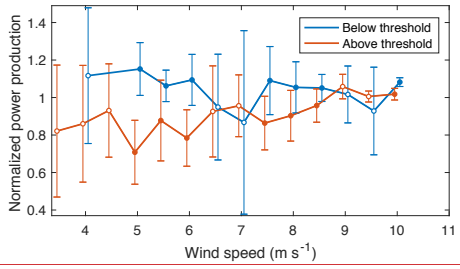

Figure 16. Mean normalized power production (turbines A, B, C and D) of observations above and below the α/β threshold for speed shear between 0.3 – 0.4 during the morning transition (0600 – 0900 LT). Filled circles are statistically distinct. Errorbars represent one standard deviation from the mean.

5 Discussion and Conclusions

Directional wind shear at the test site showed more veering cases than backing cases (Figure 7a) and a predominance of increasing wind speed with height (Figure 7b), as would be expected from the balance between Coriolis, pressure gradient, and frictional forces in the atmospheric boundary layer (Holton and Hakim, 2013). Furthermore, the largest shear values occurred between 40 m and 60 m above ground level (Figure 8), as would also be expected given that turbulent fluxes increase near the surface, causing larger wind vector rotation and speed reduction. However, cases where wind speed decreased between 40 m and 120 m evidenced the greatest rate of change between 80 m and 100 m above the surface (Figure 8b). These observations usually took place at low wind speeds during the middle of the day, where a highly convective boundary layer produces near-zero shear in the lower rotor layer.

Shear also depended on time of day (Figure 9). The observed diurnal pattern is consistent with daily radiative flux cycles. The advent of shortwave radiation from the sun at dawn drives convective air plumes from surface heating causing the largest rate of shear decrease. Rising air parcels transport air with similar zonal and meridional speed components across the rotor layer, decreasing wind shear. As the sun continues to heat the surface through the day, the convective atmosphere is strengthened, and wind direction and speed shear tend to stabilize. Once the short-wave radiative flux ceases at dusk, atmospheric stratification develops, evident from increasing shear values. A previous study in this same site found stable stratification to develop at 1900 local time, and strong veering and speed shear to develop after the evening transition (Lee and Lundquist, 2017). Median nighttime direction and speed (above 4 m s^{-1}) shear were at least 1.8 and 2.3 times larger, respectively, than daytime (Figure 10), consistent with decoupled surface and residual layers within the atmospheric boundary layer. The upper portion of the ABL starts decoupling from that close to the ground as convective turbulent fluxes no longer maintain homogeneity in the atmosphere. Vanderwende et al. (2015) found strong, persistent low-level jets during nighttime

Deleted: a

Deleted: (Holton and Hakim, 2013). Furthermore, the largest directional shear values occurred between 40 m and 60 m above the surface (Figure 6b),

Deleted: near the ground

Deleted: Directional shear depends

Deleted:) as well as wind speed (Figure 8).

Deleted: short-wave

Deleted: directional

Deleted: directional

Deleted: keeps shining

Deleted: directional

Deleted: tends

Deleted: directional

Deleted: directional

Deleted: was

Deleted: ,

at this site, which tend to further increase shear compared to daytime cases. Changes in wind direction and speed with height tended to increase throughout the night, suggesting that the rotor-layer never equilibrated during nighttime.

Though speed and direction shear in the boundary layer have equivalent forcing mechanisms, they displayed opposite relationships with increasing wind speeds (Figure 10). Convective conditions, typically with low speed shear, usually occurred at low wind speeds (Figure 12), where large direction shear was more likely (Figure 11). Large convective eddies cause a fluctuation of the meridional and zonal speed components (large direction shear), but mean horizontal wind speeds remain almost unchanged (small speed shear). Figure 12 suggests that a stratified layer, which entails large wind speed shear, primarily occurred near rated speeds. Decoupled laminar flow through the rotor layer results in low direction shear, whereas winds accelerate toward supergeostrophic speeds (large speed shear).

Nevertheless, a monotonic relationship between speed and direction shear existed for similar hub-height wind speed regimes (Figure 13). As wind profiles evolved for constant hub-height speeds, both shear parameters developed congruently due to the force balance in the boundary layer. Large surface stress reduces wind speed near the ground and results in cross-isobaric flow toward low pressure. At higher altitudes above ground level, the surface stress is lower, and the wind is geostrophic. In between these heights, the variation of speed and direction with height is described by the Ekman spiral, where wind vectors must increase in magnitude and rotate clockwise (counterclockwise) in the northern (southern) hemisphere to couple friction-driven surface winds with near-frictionless winds aloft (Stull, 1988). Further, when the surface stress decreases following radiative fluxes, inertia causes the wind to accelerate and the Coriolis force turns the wind vector clockwise (northern hemisphere) in time (Stull, 1988). The opposite case occurs with increasing surface stresses.

The combined effect of speed and direction shear on turbine performance displayed a linear threshold (given in Eq. (4)) that separates under- and overperformance at this wind farm (Figure 14). Several models have shown that power law exponents between 0 and 0.33 result in lower available power over the whole rotor area (e.g. Antoniou et al., 2009; Bardal et al., 2015). Also, as the wind vector turns with height the magnitude of the projected velocity decreases following a cosine function, causing a reduction in available power. Here, we found slight overperformance for wind shear combinations below the α/β threshold and $0 < \alpha < 0.33$, suggesting turbine blades' efficiency increased for these speed and direction shear ranges.

Large wind veering combined with small speed shear resulted in wind turbine underperformance (Figure 14). In contrast, overperformance occurred for large speed shear and small changes in wind direction with height. Observations exceeding the α/β threshold suggest that large direction shear undermined turbine operation as mean normalized performance remained below 0.96. Cases below the threshold demonstrated some underperformance (0.89 for $0.3 < \alpha < 0.4$, and direction shear between -0.1 deg m^{-1} and 0 deg m^{-1}) compared to mean operating conditions, however, mean 10-min normalized power production remained above 1 and almost three out of five observations presented overperformance. Turbine simulations using a linear wind speed and direction change across the rotor layer by Walter et al. (2009) displayed similar results, showing small power gains for little direction shear and large speed shear. However, they found the greatest power depletion for large speed shear ($\alpha = 0.35$) and counterclockwise direction shear (-0.472 deg m^{-1}), whereas our observations revealed the most detrimental conditions to be at very large veering values. Dissimilar results may be due to the scarce number of backing cases that were

Deleted: directional

Deleted: tend

Deleted: As directional shear varied through different wind speeds, its effect on turbine performance also varied. Directional wind shear exerted a larger impact on power production near cut-in wind speeds than near rated wind speeds (Figure 10). This effect amplifies as the threshold between HDWS cases and LDWS cases increases, confirming that higher directional shear has detrimental effects on performance. However, statistically significant effects on turbine power output consistently occurred only in the mid-region of the partial load regime. All examined HDWS thresholds above 0.15 deg m^{-1} exposed significant combined-turbine mean normalized power reductions for wind speeds between 5 and 8 m s^{-1}. Rareshide et al. (2009) found minor effects of wind backing on turbine performance, however these were only depicted for hub-height wind speeds of 8 m s^{-1}. Walter et al. (2009) show a similar tendency for simulations performed for 8 and 10 m s^{-1} wind speeds. Here, we considered the effects of directional shear at lower wind speed regimes and found that more detrimental effects take place below 8 m s^{-1}. ¶
In distinguishing the effects of HDWS from LDWS using a threshold of 0.225 deg m^{-1}, high directional shear reduced power output by nearly 10% compared to low directional shear scenarios for wind speeds below 8 m s^{-1}. Mean and median statistical significance tests were unanimous when considering combined-turbine performance on wind speed ranges between and 5 – 8 m s^{-1}. These findings contrast results found by Bardal et al. (2015), where directional shear larger than 5º over a 100 m rotor layer (0.05 deg m^{-1}) is found to have its major effects between 9 and 11 m s^{-1}. However, their test site presented land/sea interfaces and most of the analyzed winds came from offshore and so their data likely includes the development of an internal boundary layer due to roughness changes. Also, as is evidenced in Figure 9, our data presented low directional wind shear for near rated speeds: less than 4.5% of wind speeds above 8 m s^{-1} presented directional shear above 0.225 deg m^{-1}. In addition, directional shear in this site proves to be a major factor affecting turbine performance as 11% of partial load power production took place during HDWS atmospheric conditions between 4 and 8 m s^{-1} wind speeds.¶
Wind backing, as opposed to wind veering, was not found to affect performance in this dataset. High wind veering dominated over backing and revealed significant mean combined-turbine normalized power reductions for 4 – 8 m s^{-1} wind speeds. Rareshide et al. (2009) only found positive directional shear to reduce performance for 0.2 wind shear exponents and veering above 0.25 deg m^{-1}, whereas backing always resulted in underperformance. However, as was noted above, their results only considered 8 m s^{-1} wind speeds. Turbine performance simulations using a linear wind speed and direction change across the rotor layer by Walter et al. (2009), however, depicted slight underperformance (around 2 – 4% power change) for wind veering greater than 0.2 deg m^{-1} and wind shear exponents near 0.3. Previous studies near this site (Walton et al., 2014) have shown power-law exponents around 0.4 to be dominant during nighttime in June, July and August; thus, the significantly larger effects found in this study may also be driven by a simultaneous large wind speed shear.¶

recorded throughout the campaign. In addition, the combined effect of speed and direction shear in this site proved to be a major factor affecting turbine performance as 54% of partial load power production took place during above-threshold atmospheric conditions.

For a given value of directional shear, as quantified in 0.1 deg m^{-1} intervals, increasing the speed shear boosted the turbine performance (Figure 14). Normalized performance revealed a positive trend for each 0.1 deg m^{-1} direction shear bin as the rate of change of wind speed with height grew in magnitude. Hunter at al. (2001) reports similar results, whereby a growing magnitude of the wind vector caused a positive change in turbine power production for most wind speed regimes below rated speed. Simulations by Rareshide et al. (2009) indicate a power reduction for shear exponents between 0 and around 0.5, however observational data in their study coincides with our results for large veering and backing cases. Bardal et al. (2015), though, encountered the opposite for wind speeds in the middle of the partial load regime, possibly caused by the development of an internal boundary layer due to roughness changes at their test site owed to land/sea interfaces. Simulations by Wagner et al. (2010) displayed similar results as Bardal et al. (2015): they found a decrease in turbine power production for increasing speed shear and wind speeds above 5 m s^{-1}. Dissimilar theoretical and experimental results have been previously reported (Hunter et al., 2001). Further, though our findings indicate overperformance for rising power law exponents, the rate of increase in normalized power was smaller for large speed shear, possibly suggesting a decrease in turbine efficiency akin to simulations by Antoniou et al. (2009). In addition to differences in boundary-layer structure (like the internal boundary layer of Bardal et al. (2015)), we must point out that differences in types of turbines, turbine blade design, and turbine control algorithms may influence these results.

For a given value of speed shear, as quantified in 0.1 power law exponent intervals, increasing the directional shear resulted in turbine power depletion at this wind farm (Figure 14). Normalized performance revealed a negative trend (around -0.04 per increase in 0.1 deg m^{-1} of direction shear) for all 0.1-power law exponent bins as the change of wind direction with height grew in magnitude. Likewise, blade-element modelling using FAST evidenced decreasing turbine performance for increasing wind veer for all speed shear exponents between 0 and 0.6 (Walter et al., 2009). Conversely, Rareshide et al. (2009), looking exclusively at 8 m s^{-1} wind speeds, only reported underperformance for speed shear exponents around 0.2 and veering near 0.25 deg m^{-1}. Our results suggest more notable underperformance to occur for larger direction shear values, which were not considered in their study. Contrasting results between Walter et al. (2009) and Rareshide et al. (2009), and our findings for backing cases between $0 < \alpha < 0.6$ may be due to much less frequent and smaller numerical values compared to wind veering in our dataset. Simulations by Wagner et al. (2010) depict similar results, yet slight underperformance also occurred for veering values above 0.2 deg m^{-1} and wind speeds above 8 m s^{-1}.

Small wind backing was found to have similar effects as small wind veering. The change in energy flux through the rotor disc and turbine blades' efficiency appeared to be minor for these low direction shear conditions. Our dataset only evidenced statistically distinct power production between veering and backing for two speed shear ranges, suggesting the power asymmetries found by Walter et al. (2009) and Wagner et al. (2010) did not occur at these low shear conditions. Moreover, the small mean backing numerical values for these speed shear ranges indicate additional forcing mechanisms were in place for

these underperformance observations. Not enough large backing observations were recorded to compare turbine performance against large veering atmospheric conditions.

In distinguishing the effects of high- and low-direction shear using the α/β threshold over 0.1-α ranges, large wind veer reduced power output by more than 10% compared to below-threshold scenarios for wind speeds in the middle of the power curve (**Figure** 15). The larger proportionality between shear parameters found at lower wind speeds (Figure 13) may have augmented the effect of shear on turbine performance. These findings support those found by Bardal et al. (2015), where wind veer larger than 5 deg over a 100 m rotor layer (0.05 deg m^{-1}) was found to have its major effects in the middle of the power curve, still, the affected wind speeds differ. As stated earlier, these incongruencies may be caused by dissimilar boundary layer structures given that most of the analyzed winds came from offshore in their case.

When considering power law exponents between 0.2 and 0.3, we found direction shear to exert a larger impact on power production in the middle of the partial load regime than near cut-in or rated speeds (**Figure** 15a). Most observations within this speed shear range took place between 6.5 and 8 m s^{-1} (Figure 12), corresponding to the most affected turbine performance-speed regimes. On the other hand, highly stratified atmospheric conditions, characterized by large speed shear ($0.4 < \alpha < 0.5$), evidenced statistically distinct power differences for larger wind speeds (**Figure** 15b). Likewise, most observations for this speed shear range corresponded to near-rated wind speeds. We expected mean normalized performance for above-threshold scenarios during highly stratified atmospheric conditions ($0.4 < \alpha < 0.5$) to be smaller compared to power law exponents between 0.2 and 0.3, nonetheless observational data proved opposite. Larger directional wind shear thresholds for the former cases suggested analogous underperformance, however, the mechanical turbulence that usually accompanies large speed shear may have influenced turbine operation as well. These results prove direction shear to be an important factor that influences turbine operation. Moreover, more than 35% of observations for moderate speed shear values (0.2 – 0.5) and their correspondingly statistically affected wind speed regimes of each 0.1-power law exponent bin occurred for above-threshold shear conditions.

Focusing on a period of rapidly increasing electricity demand (0600 to 0900 local time) exposed the fact that directional shear's detrimental effects preferentially occurred during this time. Mean direction and speed shear were 0.196 deg m^{-1} and 0.37, respectively. Mean normalized power reductions were larger for this time period (~20%) compared to whole-day results (~10%) for statistically distinct wind speeds between 4.5 and 10.5 m s^{-1} and speed shear between 0.2 and 0.5 (normalized power calculated for each 0.1-α bin). Further, around 22% of observations for this time presented speed shear exponents between 0.3 and 0.4, which evidenced mean normalized power reductions close to 21% for six out of the eight 0.5-m s^{-1} wind speed regimes between 5 and 9 m s^{-1} (Figure 16). Not only did wind shear occurred often during this high-demand period of the day, but it also undermined power production at this time.

The substantial power reductions and number of cases affected by the change of wind direction with height in this wind farm make directional wind shear effects critical to consider in wind resource assessment, grid integration studies, and wind turbine control algorithm design. Large veering values affected turbine performance for small and large speed shear, suggesting that aerodynamic efficiency reductions dominate the increase in energy flux over the rotor disc caused by increasing speed

Deleted: 0530

Deleted: occur

Deleted: 9

Deleted: 8

Deleted: . Mean directional wind shear in this wind speed regime was 0.1886 deg m^{-1}, and 34.76

Deleted: directional shear larger than 0.225 deg m^{-1}.

Deleted: direction

Deleted: occur

Deleted: The substantial power reductions and number of cases affected by the change of wind direction with height in this wind farm make directional wind shear effects meaningful when considering atmospheric conditions that affect wind turbines' power production. Though this study was not able to resolve conflicting results on the effects of atmospheric stability on turbine performance, it highlights the importance of considering the effects of wind direction shear. We recommend that the magnitude and incidence of large changes of wind direction with height (>0.1 deg m^{-1}) should be studied at the sites of the conflicting studies to confirm the existence of this phenomenon. Further, since directional wind shear is highly correlated with speed shear, a higher understanding of the effects of direction shear can be obtained by separating the effects of each of these conditions, but would likely require a much larger dataset. The effects of direction shear when distinguishing between the different atmospheric stability regimes should also be examined. Analyzing the effects of directional shear on stable, neutral and convective atmospheric conditions could shed light into conflicting results and help determine if site-specific factors govern these diverging findings.¶
The direction change of the wind vector with height not only affects inflow conditions for wind turbines, but also alters how wakes evolve downwind. Wakes evolving under directional wind shear conditions skew to form an ellipsoid as they are advected downstream (Abkar et al., 2016; Aitken et al., 2014; Bhaganagar and Debnath, 2014; Bodini et al., 2017; Churchfield and Sirnivas, 2018; Englberger and Dörnbrack, 2018). Churchfield and Sirnivas (2018) performed aeroelastic simulations for turbines displaced laterally compared to an upstream turbine, finding an asymmetrical power variation explained by the mean flow asymmetry across the rotor disk caused by a skewed wake. These simulations evidenced an increase in power production when wind veering was present versus a non-direction-shear condition for certain turbine locations. Fleming et al. (2019) proved this power gain by employing a successful approach to taking advantage of wakes in wind farms (wake steering), evidencing approximately 13% increase in energy on a downstream turbine. On their study, Churchfield and Sirnivas (2018) also found an asymmetrical load-behavior variation for turbines displaced laterally compared to an upstream turbine. The impacts on wake recovery, and hence power generation, and the modification of mechanical loads (Sathe et al., 2013) consequently make directional wind shear meaningful for engineering wake models and wind farm layout and operation.¶

shear values. In addition, the fact that large directional shear undermined power production here also provides an explanation for how turbine operation was undermined for stable atmospheric conditions in the Vanderwende and Lundquist (2012) study. Turbine overperformance for stratified channeled flow conditions in St. Martin et al. (2016) and Wharton and Lundquist (2012b) studies was likely augmented by low direction shear due to channeled flow in those regions.

The present work has provided insight into the impact of wind veer on clockwise-rotating wind turbines' performance for different wind shear conditions. Recent simulations suggest that the direction of turbine rotation interacts with wind veer to affect wake structures (Englberger et al., 2019). To understand the impact of the rotational direction of a wind turbine on performance, however, future field studies and simulations should incorporate counterclockwise-rotating wind turbines. Further work regarding directional wind shear in offshore locations should also be pursued. A preliminary wind resource assessment on the coast of Massachusetts by Bodini et al. (2019) demonstrated large changes in wind direction with height. Average values of 0.1 deg m^{-1} for summertime, and 0.05 deg m^{-1} for wintertime (Bodini et al., 2019) approach the threshold at which we found significant power reductions for speed shear exponents between 0.2 and 0.3. Further, they also found the summer to have low turbulence dissipation rates, thus long-propagating skewed wakes may impact power production and loads on downwind turbines.

Deleted: evidenced

Deleted: are near

Acknowledgements

The CWEX project was supported by the National Science Foundation under the State of Iowa EPSCoR grant 1101284. The role of the University of Colorado Boulder in CWEX-13 was supported by the National Renewable Energy Laboratory. The authors thank NextEra Energy for providing the wind turbine power data. This work was authored [in part] by the National Renewable Energy Laboratory, operated by Alliance for Sustainable Energy, LLC, for the U.S. Department of Energy (DOE) under Contract No. DE-AC36-08GO28308. Funding provided by the U.S. Department of Energy Office of Energy Efficiency and Renewable Energy Wind Energy Technologies Office. The views expressed in the article do not necessarily represent the views of the DOE or the U.S. Government. The U.S. Government retains and the publisher, by accepting the article for publication, acknowledges that the U.S. Government retains a nonexclusive, paid-up, irrevocable, worldwide license to publish or reproduce the published form of this work, or allow others to do so, for U.S. Government purposes.

Deleted: 5

References

Antoniou, I., Pedersen, S. M. and Enevoldsen, P. B.: Wind Shear and Uncertainties in Power Curve Measurement and Wind Resources, Wind Engineering, 33(5), 449–468, doi:10.1260/030952409790291208, 2009.

Bardal, L. M., Sætran, L. R. and Wangsness, E.: Performance Test of a 3MW Wind Turbine – Effects of Shear and Turbulence, Energy Procedia, 80, 83–91, doi:10.1016/j.egypro.2015.11.410, 2015.

van den Berg, G. P.: Wind turbine power and sound in relation to atmospheric stability, Wind Energy, 11(2), 151–169, doi:10.1002/we.240, 2008.

Deleted: Abkar, M., Sharifi, A. and Porté-Agel, F.: Wake flow in a wind farm during a diurnal cycle, Journal of Turbulence, 17(4), 420–441, doi:10.1080/14685248.2015.1127379, 2016.¶
Aitken, M. L., Kosović, B., Mirocha, J. D. and Lundquist, J. K.: Large eddy simulation of wind turbine wake dynamics in the stable boundary layer using the Weather Research and Forecasting Model, Journal of Renewable and Sustainable Energy, 6(3), 033137, doi:10.1063/1.4885111, 2014.¶

Blackadar, A. K.: Boundary Layer Wind Maxima and Their Significance for the Growth of Nocturnal Inversions, Bulletin of the American Meteorological Society, 38(5), 283–290, 1957.

Bodini, N., Zardi, D. and Lundquist, J. K.: Three-dimensional structure of wind turbine wakes as measured by scanning lidar, Atmospheric Measurement Techniques, 10(8), 2881–2896, doi:10.5194/amt-10-2881-2017, 2017.

Bodini, N., Lundquist, J. K. and Kirincich, A.: US East Coast Lidar Measurements Show Offshore Wind Turbines Will Encounter Very Low Atmospheric Turbulence, Geophysical Research Letters, doi:10.1029/2019GL082636, 2019.

Burton, T., Sharpe, D., Jenkins, N. and Bossanyi, E.: Wind energy: handbook, J. Wiley, Chichester ; New York., 2001.

Englberger, A., Dörnbrack, A. and Lundquist, J. K.: Does the rotational direction of a wind turbine impact the wake in a stably stratified atmospheric boundary layer?, Wind Energy Science Discussions, 1–24, doi:10.5194/wes-2019-45, 2019.

General Electric: GE Energy 1.5MW Wind Turbine., 2009.

Holton, J. R. and Hakim, G. J.: An introduction to dynamic meteorology, Fifth edition., Academic Press, Amsterdam., 2013.

Hunter, R., Friis Pedersen, T., Dunbabin, P., Antoniou, I., Frandsen, S., Klug, H., Albers, A., Lee, W. K., Risø National Lab and Roskilde (DK). Wind Energy Department: European wind turbine testing procedure developments. Task 1: Measurement method to verify wind turbine performance characteristics., 2001.

International Electrochemical Comission: Power performance measurements of electricity producing wind turbines, International Electrochemical Comission, Geneva, Switzerland., 2005.

Kaiser, K., Langreder, W., Hohlen, H. and Højstrup, J.: Turbulence Correction for Power Curves, in Wind Energy, edited by J. Peinke, P. Schaumann, and S. Barth, pp. 159–162, Springer Berlin Heidelberg, Berlin, Heidelberg., 2007.

Lee, J. C. Y. and Lundquist, J. K.: Observing and Simulating Wind-Turbine Wakes During the Evening Transition, Boundary-Layer Meteorology, 164(3), 449–474, doi:10.1007/s10546-017-0257-y, 2017.

Lundquist, J. K., Takle, E. S., Boquet, M., Kosovic, B., Rhodes, M. E., Rajewski, D., Doorenbos, R., Irvin, S., Aitken, M. L., Friedrich, K., Quelet, P. T., Rana, J., Martin, C. St., Vanderwende, B. and Worsnop, R.: Lidar observations of interacting wind turbine wakes in an onshore wind farm, EWEA meeting proceedings, 10–13, 2014.

Lundquist, J. K., Churchfield, M. J., Lee, S. and Clifton, A.: Quantifying error of lidar and sodar Doppler beam swinging measurements of wind turbine wakes using computational fluid dynamics, Atmospheric Measurement Techniques, 8(2), 907–920, doi:10.5194/amt-8-907-2015, 2015.

Muñoz-Esparza, D., Lundquist, J. K., Sauer, J. A., Kosović, B. and Linn, R. R.: Coupled mesoscale-LES modeling of a diurnal cycle during the CWEX-13 field campaign: From weather to boundary-layer eddies: Coupled mesoscale-LES of a diurnal cycle, Journal of Advances in Modeling Earth Systems, 9(3), 1572–1594, doi:10.1002/2017MS000960, 2017.

National Oceanic and Atmospheric Administration: NOAA Sunrise/Sunset Calculator. [online] Available from: https://www.esrl.noaa.gov/gmd/grad/solcalc/calcdetails.html, 2019.

Rajewski, D. A., Takle, E. S., Lundquist, J. K., Oncley, S., Prueger, J. H., Horst, T. W., Rhodes, M. E., Pfeiffer, R., Hatfield, J. L., Spoth, K. K. and Doorenbos, R. K.: Crop Wind Energy Experiment (CWEX): Observations of Surface-Layer, Boundary Layer, and Mesoscale Interactions with a Wind Farm, Bulletin of the American Meteorological Society, 94(5), 655–672, doi:10.1175/BAMS-D-11-00240.1, 2013.

Deleted: Bhaganagar, K. and Debnath, M.: Implications of Stably Stratified Atmospheric Boundary Layer Turbulence on the Near-Wake Structure of Wind Turbines, Energies, 7(9), 5740–5763, doi:10.3390/en7095740, 2014.¶

Deleted: Churchfield, M. and Sirnivas, S.: On the Effects of Wind Turbine Wake Skew Caused by Wind Veer: Preprint, National Renewable Energy Laboratory, Golden, CO., 2018.¶

Deleted: . and

Deleted: .: Impact of the Diurnal Cycle of the Atmospheric Boundary Layer on Wind-Turbine Wakes: A Numerical Modelling Study, Boundary-Layer Meteorology, 166(3), 423–448, doi:10.1007/s10546-017-0309-3, 2018.¶
Fleming, P., King, J., Dykes, K., Simley, E., Roadman, J., Scholbrock, A., Murphy, P.,

Deleted: K., Moriarty, P., Fleming, K., van Dam, J., Bay, C., Mudafort, R., Lopez, H., Skopek, J., Scott, M., Ryan, B., Guernsey, C. and Brake, D.: Initial Results From

Deleted: Field Campaign of Wake Steering Applied at

Deleted: Commercial Wind Farm: Part 1,

Deleted: 22

Deleted: 5

Deleted: COUPLED MESOSCALE-LES OF A DIURNAL CYCLE…

Rajewski, D. A., Takle, E. S., Lundquist, J. K., Prueger, J. H., Pfeiffer, R. L., Hatfield, J. L., Spoth, K. K. and Doorenbos, R. K.: Changes in fluxes of heat, H2O, and CO2 caused by a large wind farm, Agricultural and Forest Meteorology, 194, 175–187, doi:10.1016/j.agrformet.2014.03.023, 2014.

Rajewski, D. A., Takle, E. S., Prueger, J. H. and Doorenbos, R. K.: Toward understanding the physical link between turbines and microclimate impacts from in situ measurements in a large wind farm: Microclimates with turbines on versus off, Journal of Geophysical Research: Atmospheres, 121(22), 13,392-13,414, doi:10.1002/2016JD025297, 2016.

Rareshide, E., Tindal, A., Johnson, C., Graves, A., Simpson, E., Bleeg, J., Harris, T. and Schoborg, D.: Effects of Complex Wind Regimes on Turbine Performance, 2009.

Rhodes, M. E. and Lundquist, J. K.: The Effect of Wind-Turbine Wakes on Summertime US Midwest Atmospheric Wind Profiles as Observed with Ground-Based Doppler Lidar, Boundary-Layer Meteorology, 149(1), 85–103, doi:10.1007/s10546-013-9834-x, 2013.

St. Martin, C. M., Lundquist, J. K., Clifton, A., Poulos, G. S. and Schreck, S. J.: Wind turbine power production and annual energy production depend on atmospheric stability and turbulence, Wind Energy Science, 1(2), 221–236, doi:10.5194/wes-1-221-2016, 2016.

Stull, R. B.: An introduction to boundary layer meteorology, Kluwer Academic Publishers, Dodrecht., 1988.

Sumner, J. and Masson, C.: Influence of Atmospheric Stability on Wind Turbine Power Performance Curves, Journal of Solar Energy Engineering, 128(4), 531, doi:10.1115/1.2347714, 2006.

U.S. Energy Information Administration: U.S. Electric System Operating Data: Regional electricity demand (Midwest), U.S. Energy Information Administration. [online] Available from: https://www.eia.gov/realtime_grid/#/data/graphs?end=20180708T00&start=20180701T00&dataTypes=k&bas=00000000000g&regions=04, 2019.

Van de Wiel, B. J. H., Moene, A. F., Steeneveld, G. J., Baas, P., Bosveld, F. C. and Holtslag, A. A. M.: A Conceptual View on Inertial Oscillations and Nocturnal Low-Level Jets, Journal of the Atmospheric Sciences, 67(8), 2679–2689, doi:10.1175/2010JAS3289.1, 2010.

Vanderwende, B. and Lundquist, J. K.: Could Crop Height Affect the Wind Resource at Agriculturally Productive Wind Farm Sites?, Boundary-Layer Meteorology, 158(3), 409–428, doi:10.1007/s10546-015-0102-0, 2016.

Vanderwende, B. J. and Lundquist, J. K.: The modification of wind turbine performance by statistically distinct atmospheric regimes, Environmental Research Letters, 7(3), 034035, doi:10.1088/1748-9326/7/3/034035, 2012.

Vanderwende, B. J., Lundquist, J. K., Rhodes, M. E., Takle, E. S. and Irvin, S. L.: Observing and Simulating the Summertime Low-Level Jet in Central Iowa, Monthly Weather Review, 143(6), 2319–2336, doi:10.1175/MWR-D-14-00325.1, 2015.

Wagner, R., Courtney, M., Larsen, T. J. and Schmidt Paulsen, U.: Simulation of shear and turbulence impact on wind turbine performance, Danmarks Tekniske Universitet, Denmark. [online] Available from: http://orbit.dtu.dk/files/4550246/ris-r-1722.pdf, 2010.

Walpole, R. E., Ed.: Probability & statistics for engineers & scientists, 8th ed., Pearson Prentice Hall, Upper Saddle River, NJ., 2007.

Deleted: MICROCLIMATE WITH TURBINES ON VERSUS OFF…

Deleted: Sathe, A., Mann, J., Barlas, T., Bierbooms, W. A. A. M. and van Bussel, G. J. W.: Influence of atmospheric stability on wind turbine loads: Atmospheric stability and loads, Wind Energy, 16(7), 1013–1032, doi:10.1002/we.1528, 2013.¶

Walter, K., Weiss, C. C., Swift, A. H. P., Chapman, J. and Kelley, N. D.: Speed and Direction Shear in the Stable Nocturnal Boundary Layer, Journal of Solar Energy Engineering, 131(1), 011013, doi:10.1115/1.3035818, 2009.

Wharton, S. and Lundquist, J. K.: Assessing atmospheric stability and its impacts on rotor-disk wind characteristics at an onshore wind farm: Atmospheric stability on rotor-disk wind characteristics, Wind Energy, 15(4), 525–546, doi:10.1002/we.483, 2012a.

Wharton, S. and Lundquist, J. K.: Atmospheric stability affects wind turbine power collection, Environmental Research Letters, 7(1), 014005, doi:10.1088/1748-9326/7/1/014005, 2012b.

Deleted: Walton, R. A., Takle, E. S. and Gallus, W. A.: Characteristics of 50–200-m Winds and Temperatures Derived from an Iowa Tall-Tower Network, Journal of Applied Meteorology and Climatology, 53(10), 2387–2393, doi:10.1175/JAMC-D-13-0340.1, 2014.¶